Climate change, fire return intervals and the growing risk of permanent forest loss in boreal Eurasia

Arden L. Burrell[1,2*] *aburrell@woodwellclimate.org

Qiaoqi Sun[3,4]

Robert Baxter[3]

Elena A. Kukavskaya[5]

Sergey Zhila[5]

Tatiana Shestakova[1]

Brendan M. Rogers[1]

Kirsten Barrett[2]

1. Woodwell Climate Research Center, Falmouth, MA, United States of America
2. Centre for Landscape and Climate Research, School of Geography, Geology and Environment, University of Leicester, University Road, LE1 7RH, UK
3. Department of Biosciences, University of Durham, Upper Mountjoy, South Road, Durham, DH1 3LE, United Kingdom.
4. College of Wildlife and Protected Area, Northeast Forestry University, 26 Hexing Road, Harbin 150040, China
5. V.N. Sukachev Institute of Forest of the Siberian Branch of the Russian Academy of Sciences - separate subdivision of the FRC KSC SB RAS, 660036 Russian Federation, Krasnoyarsk, Akademgorodok 50/28.

This manuscript is a non-peer reviewed preprint submitted to EarthArXiv. This manuscript has been submitted to Science of the Total Environment. If accepted, the final version of the manuscript will be available from the Published DOI.

Abstract

Climate change has driven an increase in the frequency and severity of fires in Eurasian boreal forests. A growing number of field studies have linked the change in fire regime to post-fire recruitment failure and permanent forest loss. In this study we used four burnt area and two forest loss datasets to calculate the landscape-scale fire return interval (FRI) and associated risk of permanent forest loss. We then used machine learning to predict how the FRI will change under a high emissions scenario (SSP3-7.0) by the end of the century. We found that there is currently 133 000 km^2 at high, or extreme, risk of fire-induced forest loss, with a further 3 M km^2 at risk by the end of the century. This has the potential to degrade or destroy some of the largest remaining intact forests in the world, negatively impact the health and economic wellbeing of people living in the region, as well as accelerate global climate change.

1. Introduction

Boreal forests contain ~30 % of all of the world's forested area (Gauthier et al., 2015), ~65% of the world's forest carbon stocks (Bradshaw and Warkentin, 2015), contribute ~20 % of the world's terrestrial carbon sink (Bradshaw and Warkentin, 2015; Pan et al., 2011) and include some of the largest areas of intact forest in the world (Potapov et al., 2017). Warming rates in the boreal region are among the fastest in the world (D'Orangeville et al., 2018), which has increased vegetation productivity (Chen et al., 2016; Goetz et al., 2005; Kauppi et al., 2014; Keenan and Riley, 2018; Liu et al., 2015) and driven the expansion of boreal species to higher altitudes and north into the tundra (Brodie et al., 2019; Forbes et al., 2010; Myers-Smith et al., 2011; Suarez et al., 1999). Whilst climate change is driving the upward and northward expansion of boreal forests, there is growing concern that it is having a contracting effect along the southern boundary with the steppe biome in more water-limited forests (Guay et al., 2014; Huang et al., 2010; Koven, 2013; Payette and Delwaide, 2003).

Wildfire is one of the largest causes of stand mortality in boreal forests, a regime which has been in place for thousands of years (Johnstone et al., 2010). As a result, many regions have been in a dynamic equilibrium, whereby the amount of ecosystem carbon lost to wildfire, determined by factors such as the Fire Return Interval (FRI) and the portion of stand-replacing fires, is balanced by the rate of recovery driven by successional dynamics or self-replacement of the dominant tree species (Brazhnik et al., 2017; Brown and Johnstone, 2012). In these regions, periodic fires play an essential role in maintaining ecosystem health and biodiversity (Kharuk et al., 2021). However, in the southern limits of the boreal zone, there is growing evidence of recruitment failure (RF), where boreal tree species fail to re-establish after a stand-replacing disturbance and instead undergo a change to a steppe/grassland (Barrett et al., 2020).

Whilst the conditions that cause RF are complex and multifaceted, certain drivers such as the Fire Return Interval (FRI) and the percentage of stand-replacing fires have distinct thresholds beyond which recruitment failure is almost certain (Hansen et al., 2018; Kukavskaya et al., 2016; Stevens-Rumann et al., 2018). For example, in the first 20-30 years after a stand replacing fire, the regenerating tree species have almost no fire tolerance and have very little ability to contribute to the seed pool (See section 2.4), which is essential for robust post-fire recruitment (Cai et al., 2018; Hansen et al., 2018; Kukavskaya et al., 2016). For this reason, the interval between a stand-replacing fire and the next fire event is one of the strongest predictors of regeneration failure within the boreal zone (Kukavskaya et al., 2016; Stevens-Rumann et al., 2018; Whitman et al., 2019).

Although the global extent of recruitment failure remains entirely unquantified (Burrell et al., 2021), RF has been observed in field studies from both the Eurasian (Barrett et al., 2020; Kukavskaya et al., 2016; Shvetsov et al., 2019) and North American boreal forest (Baltzer et al., In Press.; Boucher et al., 2019; Brown and Johnstone, 2012; Hansen et al., 2018; Stevens-Rumann et al., 2018). In a study of 1538 field sites across boreal North America, post-fire RF was observed at ~10% of sites (Baltzer et al., In Press.). If RF and its associated forest loss is widespread, this poses a serious risk to the wealth of ecosystem services provided by boreal forests including timber supply, which is one of the largest industries in the boreal zone (Gauthier et al., 2015; Hansen et al., 2013). It would also negatively impact the boreal carbon sink, potentially leading to a net source, which would further amplify climate change (Chen and Loboda, 2018; Hayes et al., 2011; Lin et al., 2020).

The reason the extent of recruitment failure remains unknown is because of a lack of the data and methods needed to systematically quantify it at large scales (Burrell et al., 2021). The ideal method to measure post-fire RF would involve a large number of field sites with >30 years of records, which does not currently exist for many parts of the, often very remote, boreal zone, with the data availability in Siberia, for example, being especially low (Burrell et al., 2021). Another option for quantifying RF would be to directly detect it using remotely sensed imagery, or by proxy using remotely sensed data products to construct site-level fire histories. Such histories can indicate where the gap between a stand-replacing fire and the subsequent fire event was less than the 30-year threshold observed in field studies of recruitment (Hansen et al., 2018; Kukavskaya et al., 2016). To the best of our knowledge, there have been no studies that have done this at a large spatial scale. This is likely because performing the analysis over a large area would require high spatial resolution data with a temporal record that is longer than is currently available (Burrell et al., 2021; Chu and

Guo, 2014). Existing studies using remote sensing to look at post-fire forest recovery generally only assess recovery in the first 5 years after fire (Frazier et al., 2018). Given that site-level fire/disturbance histories extending beyond the satellite period are unavailable in most areas, landscape-scale FRI, calculated using a space for time substitution, has been used to investigate ecosystem changes driven by wildfire (Coops et al., 2018; Kharuk et al., 2021; Soja et al., 2006; Tomshin and Solovyev, 2021).

In addition, there is growing evidence that climate change has already driven an increase in the frequency, extent and severity of boreal fires, which has shortened the FRI and increased the proportion of fires that are stand replacing (Brazhnik et al., 2017; Feurdean et al., 2020; Malevsky-Malevich et al., 2008; Ponomarev et al., 2016; Tomshin and Solovyev, 2021). As the climate continues to warm, this trend is likely to continue, with the Sixth Assessment Report of the United Nations Intergovernmental Panel on Climate Change (IPCC) predicting increase in fire frequency and severity across all of Eurasia (IPCC, 2021). Given the strong link to climate change, the growing evidence of site level RF, the threat it poses to boreal carbon sink and the difficulty in measuring it over a large area, it is no surprise that a recent review of Arctic boreal science identified quantifying the extent of boreal RF as a key knowledge gap in the boreal zone (Goetz et al., In Review.).

The aim of the present study was to use freely available remotely sensed datasets to investigate landscape-scale FRI, stand replacing FRI (FRI_{SR}) and the all-cause Disturbance Return Interval (DRI) which together can be used as a proxy for RF risk and, by association, the areas most at risk of permanent biome shift in the Eurasian boreal forest. The extreme gradient boosted regression machine learning method was then used to examine the link between FRI and climate over the observed period and, in combination with future climate projections, to quantify how this risk will change over the next century.

2. Methods

2.1 Region of interest

The analysis was performed over the entire Eurasian boreal forest, a region containing ~15 M km^2 of forest dominated by a small number of tree species from four main genera, larch (*Larix*), pine (*Pinus)*, birch (*Betula*), and spruce (*Picea*) (Bartalev et al., 2004; de Groot et al., 2013; Rogers et al., 2015). Siberia contains some of the hottest and driest parts of the boreal biome and is warming faster than the global average (Burrell et al., 2021). Given the influence of fuel availability, fire season length, and fire weather, there are direct links between burned area and climatology, as well as climate changes in Siberia (de Groot et al., 2013; Kharuk et al., 2021; Tepley et al., 2018). The

Eurasian boreal biome has already experienced an increase in both the length of the fire season and a shortening of the FRI, trends that are predicted to continue with anthropogenic climate change (Malevsky-Malevich et al., 2008; Shvetsov et al., 2016). The Russian Far East and Siberian portions of the boreal zone have been the focus of notably fewer research studies than either the North American or Scandinavian boreal forest (Rogers et al., 2020), which is particularly problematic, because the climatology and current rates of warming in Siberia suggest that the changes occurring in this region may be truly indicative of the future of the boreal zone as the climate warms (Burrell et al., 2021).

To distinguish the boreal-steppe boundary, we used version 1.7 of the Hansen Global Forest Change 2000 tree cover data (Hansen et al., 2013) to mask out non-forested areas in all datasets. As this study is focused on the shift of the boreal-steppe boundary and existing static boreal forest maps may be misleading due to shifts in this boundary, we derived the boreal biome boundary using forest cover data rather than using an existing biome map. For this study we included any area located between 40° to 70° of latitude and -10.0° to 180° of longitude that had a fractional tree cover greater than 10 %. To exclude the temperate forests that occur in these regions, we then used boreal ecoregions from Dinerstein et al., (2017) with a 1° buffer to account for any uncertainties in the boundaries. Figure 1 shows the dominant land cover type and tree species over the entire domain.

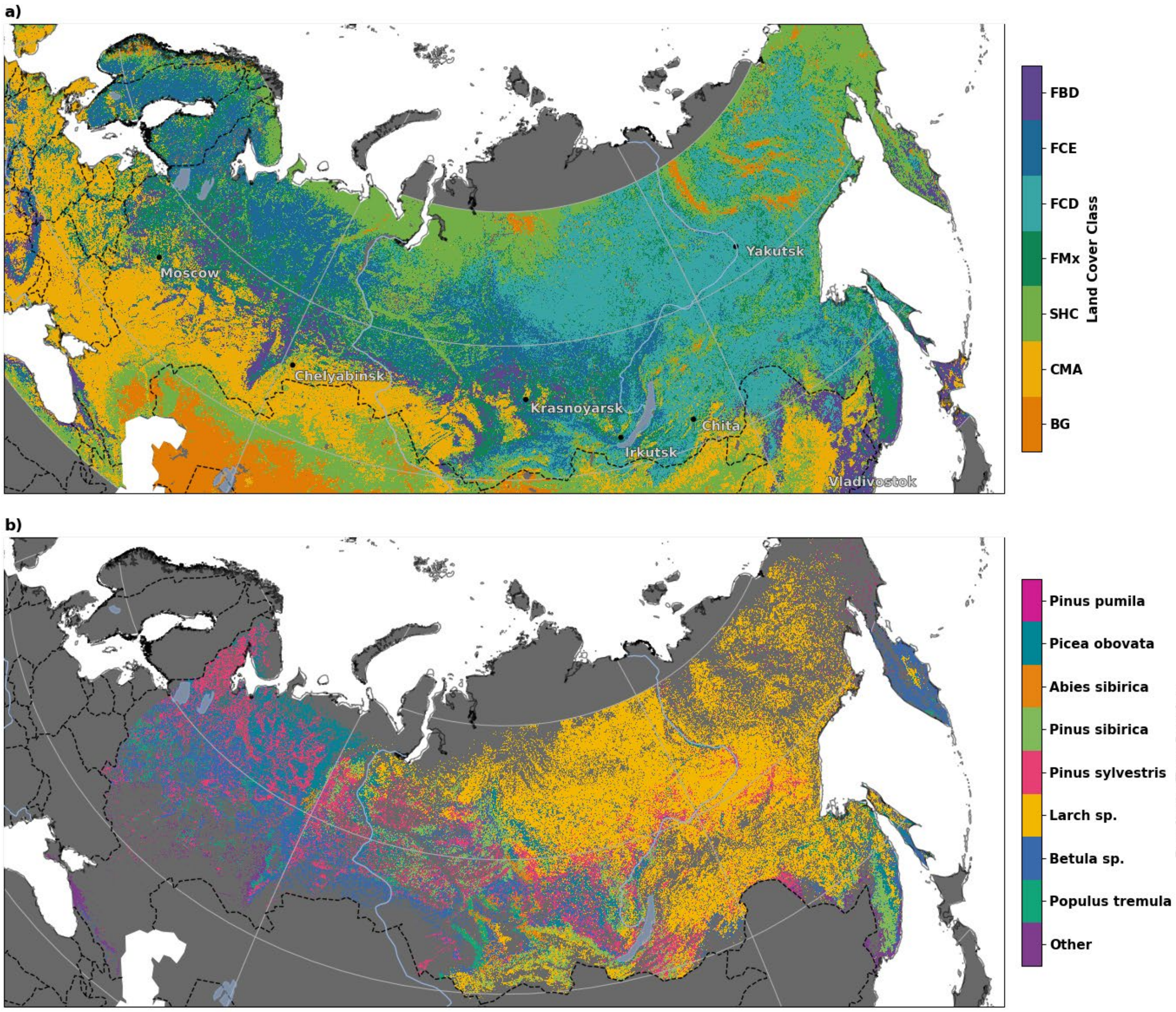

Figure 1. Land cover types. *a) The dominant land cover class in the year 2000 (FBD: Broadleaf Deciduous Forest, FCE: Coniferous Evergreen Forest, FCD: Coniferous Deciduous Forest, FMx: Mixed Forest, SHC: Shrubs and/or Herbaceous Cover, CMA: Cultivated and/or Mixed Agriculture, BG: Bare Ground). b) The dominant tree species. Data: a) GLC2000 (Bartholomé and Belward, 2005) and b) adapted from (Bartalev et al., 2004).*

2.2 Burnt Area Datasets

In order to partially control for the uncertainties and biases in any one data source, we used four global Burnt Area (BA) products to estimate Fire Return Intervals in Eurasian boreal forests. The first is the Moderate Resolution Imaging Spectroradiometer (MODIS) Collection 6 Burned Area product (MCD64A1), which has a ~500 m resolution, covers 2001 to present and is the most widely used and validated global BA dataset (Giglio et al., 2018). The second is the fourth version of the Global Fire Emissions Database 4.1 (GFED4) burned area (including small fires) (van der Werf et al., 2017), which has a 0.25-degree resolution, covers the period from 1996 to near 2017 and is mostly based on

MODIS MCD64A1 data (Randerson et al., 2017). The ‘small fires’ version of GFED4 has a correction applied to address the known bias in BA products to underrepresent the extent and frequency of smaller and/or low intensity fires (Randerson et al., 2012). The third is the European Space Agency’s Climate Change Initiative FireCCI version 5.1 (FireCCI51), which uses MODIS spectral and active fire data, has a ~250 m resolution and covers the period 2001 to present (Lizundia-Loiola et al., 2020). The fourth is the Copernicus Global Land Service Burnt Area product (CGLS-BA), which is derived from PROBA-V data, has a ~300 m spatial resolution and covers the period 2014 to present (Smets et al., 2017). The performance of CGLS-BA is expected to be worse than other products in the boreal zone because it cannot detect any spring or autumn fires north of 51°, but we included it in this study because it is the only high-resolution global BA product that is currently being updated and is entirely independent of MODIS data.

In addition to the BA products, we also used version 1.7 of the 25 m Hansen Global Forest Change (HansenGFC) dataset to examine forest loss rates (Hansen et al., 2013). HansenGFC v1.7 uses Landsat 8 for improved detection of boreal forest loss, including from fire. However, this correction is not applied to the years 2001 to 2010. To examine the rate of forest loss due to fires, we followed the procedure used by Krylov et al., (2014) and used MODIS active fire data (MCD14ML) to mask out areas where forest loss does not occur within 4 km of a fire (HansenGFC-MAF).

2.3 Calculating landscape-scale FRI

Estimating site-level Fire Return Interval (FRI) requires long-term observations from multiple fire events, typically from sediment cores, tree rings from surviving trees or long-term site monitoring; information that is not publicly available for most of the Eurasian boreal forest zone. FRI can also be calculated at regional and continental scales using space-for-time substitution, assuming homogeneity in FRI within a given grid cell at a particular spatial resolution (Archibald et al., 2013). Because all the moderate and high spatial resolution BA products currently available have insufficient temporal record for the majority of site-level FRI’s in Eurasian boreal forests, we adopted this latter convention. For the four BA datasets (GFED4, FIreCCI51, MCD64A1 and CGLS-BA), we calculated the fire frequency for each forested pixel and then applied a 1 degree moving window (excluding non-forest areas) to calculate the landscape-scale mean annual burned fraction (AnBF). The landscape FRI was then calculated by taking the reciprocal of the AnBF. This procedure was also applied to both the HansenGFC and HansenGFC-MAF to calculate the Disturbance Return Interval (DRI) and the FRI_{SR} respectively, after upscaling these products from their native 25 m resolution to 250 m (the same grid as FireCCI). For all datasets we used the full temporal record available at time of analysis (2001 to 2018 for FIreCCI51, MCD64A1, HansenGFC and HansenGFC-MAF; 1997 to 2018 for GFED4; and 2014 to 2018 for CGLS-BA) which may account for some of the differences between the estimated FRI's.

Using a space-for-time substitution to calculate FRI becomes much less accurate in areas with long FRI's (small AnBF's) (Archibald et al., 2013; Falk et al., 2007). In these areas the addition of a single fire event can make a large difference in the calculated FRI. For this reason, we only report FRI up to 10 000 years. Pixels with FRI >10 000 years were also excluded from the modelling of FRI.

2.4 Selection of critical thresholds

In the present study we used thresholds of landscape FRI as a proxy for the risk of permanent forest loss with <15 years indicating catastrophic risk and 15 to 30 years indicating high risk. These thresholds were selected based upon information from Scots Pine (*Pinus sylvestris*) stands, which have been studied in the context of recruitment failure and represent the dominant tree species in parts of the Eurasian boreal forest with the highest levels of drought and shortest FRI's (Shvetsov et al., 2019) which means it represents a reasonable lower bound of the FRI survivability of boreal tree species. Whilst stand-replacing fires temporarily reduce the risk of subsequent fire events by reducing fuel loads (Bernier et al., 2016; Beverly and Beverly, 2017; Erni et al., 2018; Walker et al., 2020), this effect appears to be relatively short-lived in Siberia because of the rapid recovery of flammable understory grasses (Kukavskaya et al., 2014), with studies showing that wildfire can occur in a forest of any stand age, composition or canopy density (Brazhnik et al., 2017; Hansen et al., 2013; Kukavskaya et al., 2016). Given this, and assuming that a proportion of fires are stand-replacing (discussed below), the landscape FRI indicates how long a forest has between a stand replacing fire and the next fire event.

We used two primary sources of ecological information on *Pinus sylvestris* to establish our risk thresholds. The first is the relationship between stand age and seed production, and the second is the relationship between stand age and fire-induced tree mortality. Whilst high severity crown fires result in high to total mortality of trees regardless of age and DBH, the probability of mortality for a tree in low-severity surface fires is directly associated with its width, or diameter at breast height (DBH): for example the probability of fire-induced mortality is 80 to 100 % for trees with DBH <10 cm, 14 % for DBH from 10 to 20 cm and 1.4 % for tress with a DBH of 40 to 50 cm (Kukavskaya et al., 2014; Linder et al., 1998). As for the relationships between stand age and seed production, it generally takes between 5 and 15 years after a stand-replacing fire for trees to produce seeds that begin to replenish the seedbank (Sullivan, 1993; Wright et al., 1967). This initial seed production is generally very limited, with the first large seeding events not occurring until the trees reach 25 to 30 years old (Broome et al., 2016).

Trees less than 15 years old generally have a DBH < 10 cm, meaning any fires that occur within that period will kill almost all the saplings, and with little to no seedbank, a transition to non-forested ecosystem is almost guaranteed unless the stand is immediately adjacent to a seed source (Chmura et al., 2012; Kukavskaya et al., 2014; Linder et al., 1998). Multiple field studies have observed recruitment failure if an area burns again <15 years after a stand-replacing fire (Kukavskaya et al., 2016, 2016; Shvetsov et al., 2016). While the stand age vs DBH relationship varies considerably between regions, in general stands 30 years old will have DBHs between 10 and 20 cm, which means they have ~50 % chance of surviving a low-severity surface fire (Linder et al., 1998; Sidoroff et al., 2007; Sullivan, 1993). We chose 15 to 30 years as our second critical threshold due to both the high mortality rate and lower seed availability before the first mass seeding event.

Using these landscape FRI thresholds as a proxy for post-fire recruitment failure and permanent forest loss is predicated upon three key assumptions. The first is that Scots pine represents a reasonable lower bound of the FRI survivability of boreal tree species. Scots pine is one of the dominant species in regions of the boreal zone with the shortest FRI's (Kukavskaya et al., 2016), which suggests a fire regime that excludes Scots pine is highly likely to exclude all other boreal tree species such as larch (*Larix* spp.) and dark taiga (*Picea* and *Abies* spp.) (Schulze et al., 2012). Applying the procedure detailed above to larch gives FRI thresholds that are equal to, or greater than, those for Scots pine. In addition, our thresholds are consistent with those found in studies of post-fire recruitment failure in similar ecosystems with different dominant species across the globe (Baltzer et al., In Press.). For example, in a study of recruitment failure in the alpine region of the continental USA, the serotinous lodgepole pine (*Pinus contorta*), a species whose first large seeding event occurs at 15 years old (Broome et al., 2016), only failed to establish when fire return intervals were <20 years and stands were far (>1 km) from a seed source (Hansen et al., 2018).

The second key assumption is that the fire observed in the BA data for a given area includes some stand replacing fires. Whilst most fires in the Siberian boreal forests are surface fires (Rogers et al., 2015), if all the fires observed in an area are low severity surface fires in mature forests with little to no fire-induced stand mortality, then FRI cannot be used a proxy for ecosystem risk. Whilst not common in most coniferous forests, this non-stand-replacing fire dynamic has been observed in the broadleaf forest along the boreal-temperate boundary (Krylov et al., 2014; Schulze et al., 2012). A similar dynamic has also been observed in some mature Scots pine forest stands in southern Siberia with FRI's of 20 to 40 years, but less than 10% of fires being high mortality crown fires (Kharuk et al., 2021). To account for the influence of low-severity surface fires versus stand-replacing fires, we compared the DRI and FRI_{SR} from HansenGFC and HansenGFC-MAF data, respectively. In the Eurasian boreal zone, conifer species generally have a FRI of between 30 to 50 years and FRI_{SR} around 200 years (120 to 300 years), though FRI_{SR}'s as low as 60 years have been observed in some of the southern boreal regions (Kharuk et al., 2021, 2016; Schulze et al., 2012). We used the DRI and FRI_{SR} thresholds of <60 and <120 years along with the FRI thresholds of <15 and < 30 years to determine the risk of forest loss, with an area only considered at high or extreme risk if both the FRI is < 30 years and the FRI_{SR} is <120 years. The full risk criteria are described in Table 1.

Table 1 *Thresholds used to determine forest loss risk. All number represent years.*

	FRI_{SR}<60	**FRI_{SR} 60-120**		**FRI_{SR}>120**		
	DRI<60	**DRI<60**	**DRI 60-120**	**DRI<60**	**DRI 60-120**	**DRI>120**
FRI<15	Extreme Risk (fire)	Extreme Risk (fire)	Extreme Risk (dist)	Extreme Risk (dist)	Extreme Risk (fire)	Moderate Risk (fire)
FRI 15-30	Extreme Risk (fire)	Extreme Risk (dist)	High Risk (fire)	Extreme Risk (dist)	High Risk (dist)	Moderate Risk (fire)
FRI>30	Moderate Risk (fire)	Moderate Risk (dist)	Moderate Risk (fire)	Moderate Risk (dist)	Moderate Risk (dist)	Low Risk

The final assumption is that errors in the BA products do not have high commission errors. Accuracy assessments of BA products have found large errors with a strong omissions bias and a tendency to greatly underrepresent low severity surface fires in the boreal zone (Brennan et al., 2019; Giglio et al., 2018; Humber et al., 2019; Lizundia-Loiola et al., 2020). This would indicate that the actual landscape-scale FRI might be significantly shorter than that found in this study. We also performed a small, independent, accuracy assessment at 50 field sites in the Zabaikal region of southern Siberia (described below).

2.5 Assessing the accuracy of RS BA products

Unlike boreal forests in North America and Scandinavia, Siberia has a well-documented lack of site-level burn scar mapping that can be used to validate BA products (Burrell et al., 2021). This is especially true in parts of the former Soviet Union where, in some locations, the memory of individual foresters constitutes the only records of fires.

To assess the BA products, we estimated site-level fire histories at 50 existing field sites located in southern Siberia (Barrett et al., 2020) using Google Earth Engine to identify available Landsat images. For each site a time lapse video was built showing the R-G-B scenes as well as near infrared (NIR)-R-G and shortwave infrared (SIR)-NIR-R false colour composites. We used these videos to record every fire or disturbance event at the site, as well as within a 1 km-by-1 km bounding box around each site. To reduce the risk of user-error, every site was assessed by at least two people independently. Examples of a burn in these images are included in Supplementary Figure 1. We compared this user generated fire history with the BA products and scored the products using the following criteria: Correct Detection (CD) is a burn that is apparent in both the user generated and BA product (±1 year to account for gaps in the Landsat record). A Spatial Underestimation (SU) is when the BA product detects a fire in the 1 km x 1 km, but not in the pixel that includes the site, whilst the user generated fire history has the fire impacting the site. A Spatial Overestimation (SO) is the opposite of a Spatial Underestimation, with the manual fire history recording a fire in the box but not impacting the site, whilst the BA product detects a fire disturbance at the site. A False Negative (FN) represents a fire in the manual fire history but not in the BA data. A False Positive (FP) represents a fire in the BA that could not be observed in the manual fire history. A similar approach was used to assess HansenGFC, though all stand loss disturbances were considered, and for HansenGFC-MAF, in which case only stand loss driven by fire events, was included. GFED4 was not assessed because its spatial resolution is too coarse for site-level accuracy assessments.

The main limitation to our time-series based approach to identifying burned areas is that, whilst it is easy to detect stand-replacing fires in the Landsat images because the impacts are apparent for years after the actual burn, gaps in the Landsat record mean it is easy to miss low severity understory or grassland fires. This is a potential problem because forests that are regenerating after a stand-replacing fire are dominated by grasses (Kukavskaya et al., 2014) and are spectrally similar to grasslands. As such, our ability to assess Correct Detections (CD) of burned area and False Negatives (FN) is much higher than our ability to assess False Positives (FP), with a portion of the FP’s we observe likely being correct detections that could not be seen in the available Landsat images due to low fire severity.

2.6 Modelling the relationship between FRI and the climatology

We fitted an extreme gradient boosted machine learning model (Chen and Guestrin, 2016) to examine the relationship between FRI and climatology and to predict how FRI may change into the future. To look at the relationship between FRI and climatology, as well as to quantify the rate of climate change, we used TerraClimate gridded monthly temperature and precipitation data (Abatzoglou et al., 2018) as well as the TerraClimate predicted future climate (Qin et al., 2020). TerraClimate is a ~4 km global dataset of monthly climate variables created by combining multiple existing gridded and remotely-sensed climate data products (Abatzoglou et al., 2018).

To calculate our observed climatology, we used TerraClimate precipitation and temperature data (Abatzoglou et al., 2018). For each year we calculated the accumulated precipitation and the monthly mean temperature for the meteorological seasons (DJF, MAM, JJA, SON). The seasonal climatology was then calculated by taking the mean over the 31 years from 1985 to 2015. This time period was chosen because it is long enough to account for natural climate variability (Burrell et al., 2020), has a significant overlap will all the BA datasets, and is directly comparable to the TerraClimate predicted future climate (Qin et al., 2020).

To calculate the relationship between FRI and seasonal climatology, the climate dataset was resampled to the same grid as the FRI dataset being tested using a second order conservative remapping (CDO, 2018). Then we first applied the same 1^{o} x 1^{o} moving window to climate data as we used to calculate the FRI. To avoid training and testing the machine learning models on spatially autocorrelated data, one pixel was selected from each 1^{o} x 1^{o} grid cell. We then excluded areas with less than 10 % forest cover as well as areas with landscape FRI >10 000 because of the low confidence in these values for the reasons detailed in section 2.3.

We used mean Annual Burnt fraction (AnBF = 1/FRI) as a dependent variable because initial trials showed better model performance predicting AnBF and then converting to FRI compared to models that predict FRI directly. This is probably because machine learning methods perform better on variables that are scaled between 0 and 1 (Pedregosa et al., 2011). For independent variables, we used the seasonal precipitation and temperature climatology as well as the mean tree cover fraction in the year 2000 derived from Hansen GFC dataset (Hansen et al., 2013). These independent variables were pre-processed using a Quantile Transform. We then used python's scikit-learn package (Pedregosa et al., 2011) to perform an 80:20 test-train split with the 20 % remaining withheld data to assess out-of-sample accuracy.

To model the relationship between FRI and climatology, we applied two machine learning approaches. The first was a simple multivariate regression implemented using the scikit-learn python library (Pedregosa et al., 2011), and the second was as an Extreme Gradient Boosted regression implemented using XGBoost (Chen and Guestrin, 2016). The accuracy of the models was assessed by calculating the R^2 on the fully withheld testing values. We then applied these trained models to every pixel at the native resolution of the BA product. This process was undertaken using all four of the BA datasets with the importance of different variables determined using Feature Importance and Permutation Importance tests.

2.7 Determining the climate change-driven trends and estimating future FRI

To estimate future FRI, we also used the recently developed TerraClimate predicted future climate (Qin et al., 2020), which uses a 23-member climate models ensemble to generate a realistic climate dataset for the period 2085 to 2115 under Shared Socioeconomic Pathways (SSP)3 – 7.0 emissions. Because of the known issues with CMIP model predictions of precipitation, we also created three predicted climatologies for the periods 2015 to 2045, 2045 to 2075, and 2085 to 2115, based on the current climate change-driven trends in precipitation and temperature. In addition, we calculated the future fire-induced forest loss risk using the predictions of FRI and the fire risk criteria detailed in Table 1. The calculation of future forest loss risk assumes that the proportion of fires that were stand replacing remained constant though time for a given location.

Calculating the climate change-driven trend in regions with high natural climate variability, such as the boreal steppe transition zone in Siberia, requires removing the inherent interannual and inter-decadal climate variability (Burrell et al., 2020, 2019). To do so, we used the process outlined in Burrell et al. (2020), whereby a 20-year leading edge moving window was applied to each pixel to remove interannual climate variability. A Theil-sen Slope estimator (Theil, 1950) was then applied to calculate the climate change-driven shift in seasonal temperature over the period 1985 to 2015 with a Spearman's rank correlation co-efficient test used to measure statistical significance for each pixel (Yue et al., 2002). The Benjamini–Hochberg procedure was then applied to these p-values to control for False Discovery Rate (FDR) ($\alpha_{FDR} = 0.10$), which accounts for multiple testing and spatial autocorrelation issues (See (Wilks, 2016) for details). We then used the observed climate change driven trend and the significant trends to estimate future climatology. Non-significant trends were not included. All the climatology datasets were prepared in the same manner as detailed in section 2.6, and the models trained over the observed period (1985 to 2015) were applied to create estimates of future FRI.

3. Results

3.1 Current Fire Return Interval

The median (1st, 99th percentile) FRI over the Eurasian boreal forest was 446 yrs (20 yrs, >10,000 yrs) for GFED4, 549 (17 yrs, >10,000 yrs) for MCD64A1, 501 (9yrs, >10,000yrs) for FireCCI51 and 319 yrs

(21 yrs, >10,000 yrs) for CGLS-BA. Looking at the areas with the shortest FRI's, our results indicate that between 0.2% and 2.4% (GFED4: 32,011 km^2, MCD64A1: 65,356 km^2, FireCCI:225,932 km^2, CGLS-BA: 21,114 km^2) of the Eurasian boreal zone that was forested in 2000 has experienced an FRI <15 years. In addition, there is a further 2.2% and 3.3% of forests with FRI's between 15 to 30 years (GFED4: 215,612 km^2, MCD64A1: 269,934 km^2, FireCCI: 255,931 km^2, CGLS-BA: 347,181 km^2). In areas with a stand-replacing fire regime, a FRI of <30 years places forests at high risk of post-fire recruitment failure and forest loss whilst an FRI of <15 years indicates that a region has likely already experienced permanent forest loss or will in the next few decades assuming a portion of the fires are stand-replacing (See section 2.4).

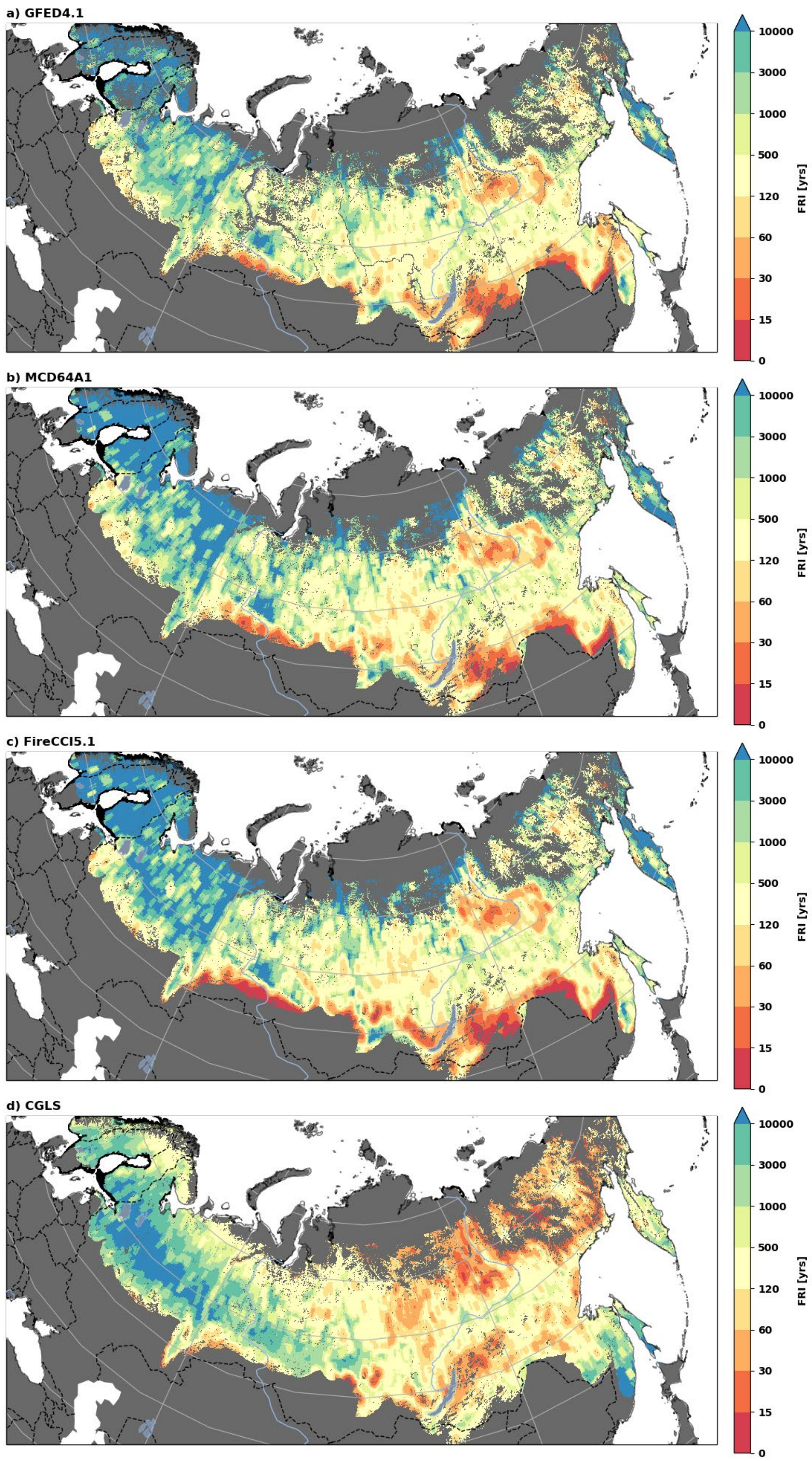

Figure 2 Maps of the landscape-scale Fire Return Interval (FRI) *in years calculated using a 1^o x 1^o moving window applied to four Burnt Area (BA) datasets: a) GFED4; b) MCD64A1; c) FireCCI51, and d) CGLS-BA. Non-Boreal Forest regions are masked in grey.*

To determine which parts of Eurasia experienced a disturbance-recovery regime, we calculated the stand-replacing Fire Return Interval (FRI_{SR}) (Figure 3a), the all-cause Disturbance Return Interval (DRI) (Figure 3b) using the Hansen global forest cover dataset, and the proportion of fires that are stand-replacing (Figure 3c). the DRI with fire removed in included in Supplementary figure 4 For FRI to be a reliable proxy for risk of forest loss, the Burnt Area (BA) must include stand-replacing fires, not just understory fires with little stand mortality (See section 2.4 for additional explanation). Over the Eurasian boreal forest, the median (1^{st}, 99^{th} percentile) FRI_{SR} was 1302 yrs (59 yrs, >10,000 yrs). In 40% of areas, 100% of the observed fires were stand replacing, with an area weighted mean stand replacing fire percentage of 69% across the entire domain. The all-cause Disturbance Return Interval (DRI) was 367 yrs (52 yrs, >10,000 yrs).

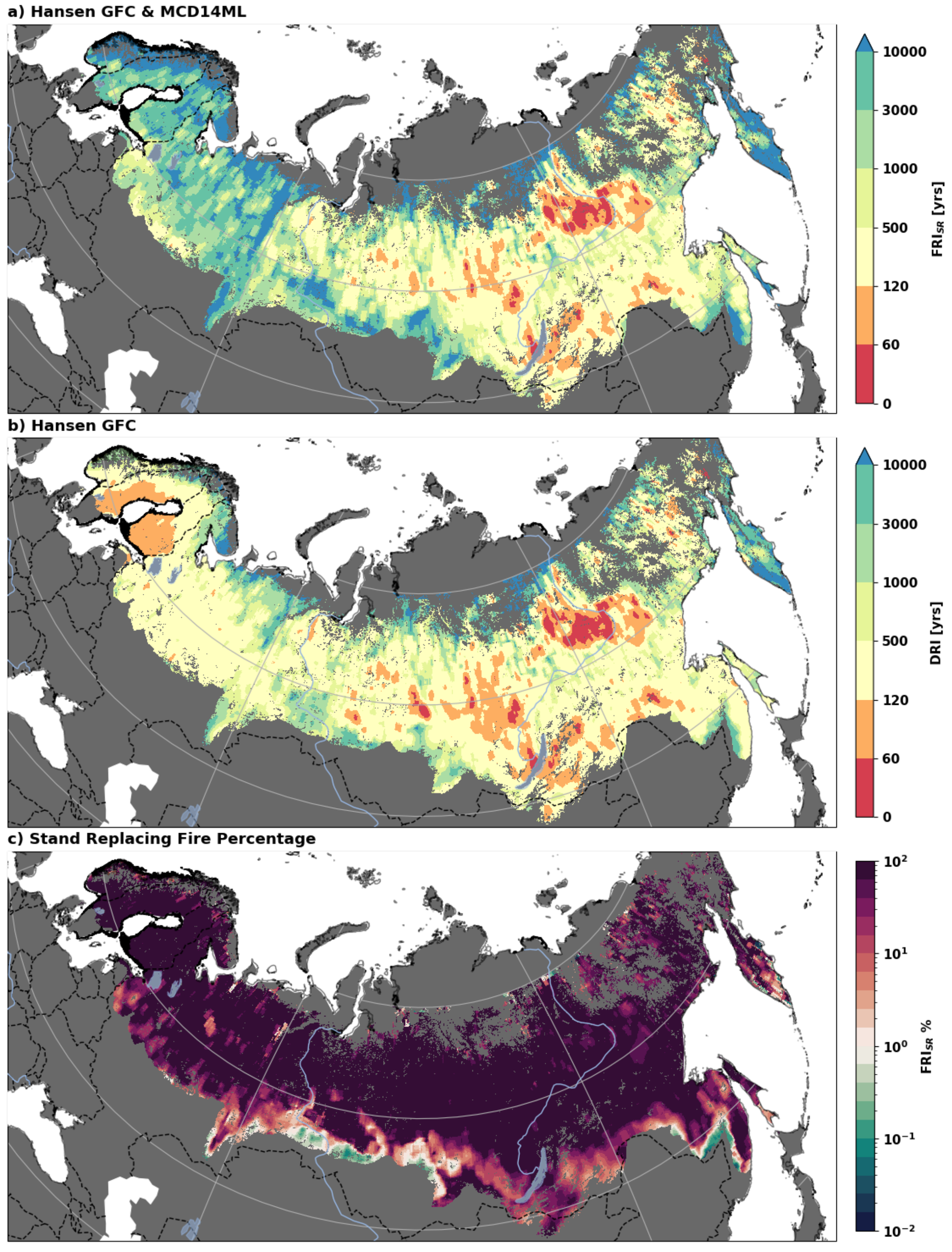

Figure 3 Rates of Forest loss *a) The stand-replacing Fire Return Interval (FRI_{SR}) calculated using HansenGFC-MAF (Krylov et al., 2014); b) the Disturbance Return Interval (DRI) calculated using HansenGFC (Hansen et al., 2013); c) The percentage of fires that are stand-replacing calculated by dividing the FireCCI5.1 mean annual burn fraction with the HansenGFC-MAF mean annual burn fraction. Note: Percentage is shown on a log scale.*

Figure 4 shows the fraction of fires that are stand replacing for each dominant tree species. In the pine, larch and spruce forests, which dominate in the eastern half of the continent, the only fires detected were stand-replacing in more than 40% of areas, with only a small fraction of areas having a high proportion of non-stand-replacing fires. By contrast, Fir, Birch and aspen, as well as the Maple, Linden, Beech and Oak which make up the *other* category in Figure 4, all have large proportions of their areas with low rates stand replacing fires.

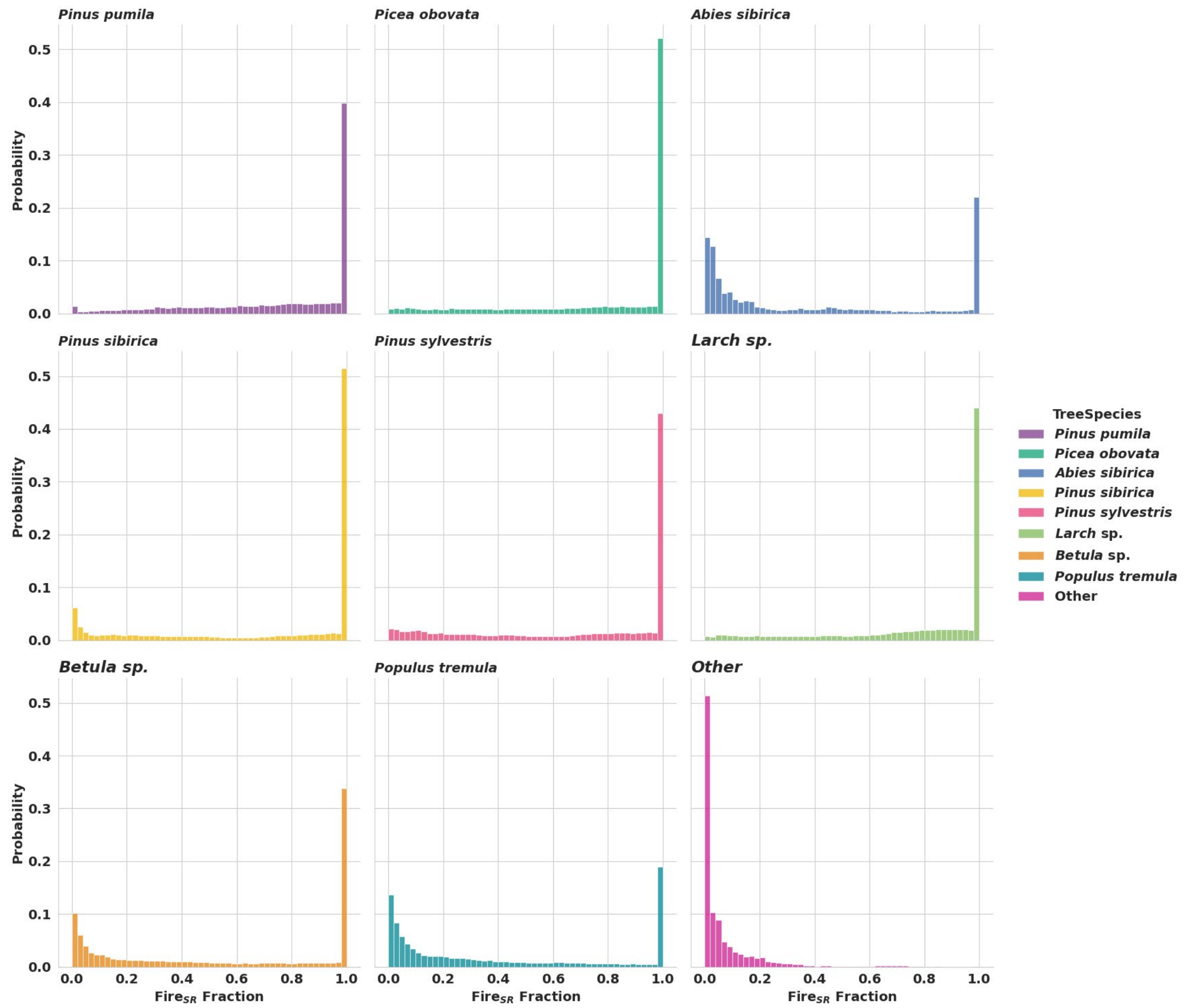

Figure 4 Stand-Replainng fire fraction. *Binned probabilty distribution histogragm of the stand-repacing fire fraction (FireCCI5.1 mean annual burn fraction / HansenGFC-MAF mean annual burn fraction) for the dominant tree species. Areas where tree species data were unavilable, or where FireCCI5.1 FRI> 10,000 yrs, were excluded.*

3.2 Accuracy Assessment and Uncertainties

For FRI to be usable as an indicator of the risk of permanent forest loss, the BA products used to calculate FRI cannot have a significant overestimation bias in burnt area. Looking at the large-scale patterns, FRI's calculated from the three MODIS-derived BA datasets (GFED4, MCD64A1, FireCCI51) show similar spatial patterns with the shortest FRI's observed along the southern boundary of the Eurasian boreal forest, as well as the forests around Yakutsk. There is less agreement between CGLS-BA and the MODIS-derived BA products, with large differences along the northern tundra/boreal border, as well as in Far East along the China-Russia border north of Vladivostok (Figure 2). The differences in the south-eastern portion of the study are unsurprising because CGLS-BA has a much shorter record and cannot capture fires during spring or autumn north of 51°N (Smets et al., 2017). This is problematic because in south-eastern Siberia the fire season starts as early as March (Feurdean et al., 2020; Hayasaka et al., 2020; Shvetsov et al., 2019). However, this cannot explain why CGLS-BA has much shorter FRI's in north-western Siberia. Previous assessments of BA accuracy noted the tendency for CGLS-BA to overestimates burns in this region (Humber et al., 2019).

To assess the accuracy and bias in the datasets, the fire histories obtained from the three high-resolution BA products (MCD64A1, CGLS-BA and FireCCI51) and the two forest-loss datasets (HansenGFL, and HansenGFC-MAF) were compared to manually generated fire histories at 50 existing field sites in south-eastern Siberia (Figure 5). We find that all three BA products have low accuracy, with the most accurate dataset (FireCCI51) only correctly detecting fires *ca*. 34 % of the time. This is in line with previous assessments of the accuracy of BA products that have shown that, whilst performance in boreal forest is better than other ecozones (Humber et al., 2019), the rates of both omission (False Negative) and commission (False Positive) errors are generally high, and omissions exceed commissions in most studies (Brennan et al., 2019; Giglio et al., 2018; Humber et al., 2019; Lizundia-Loiola et al., 2020).

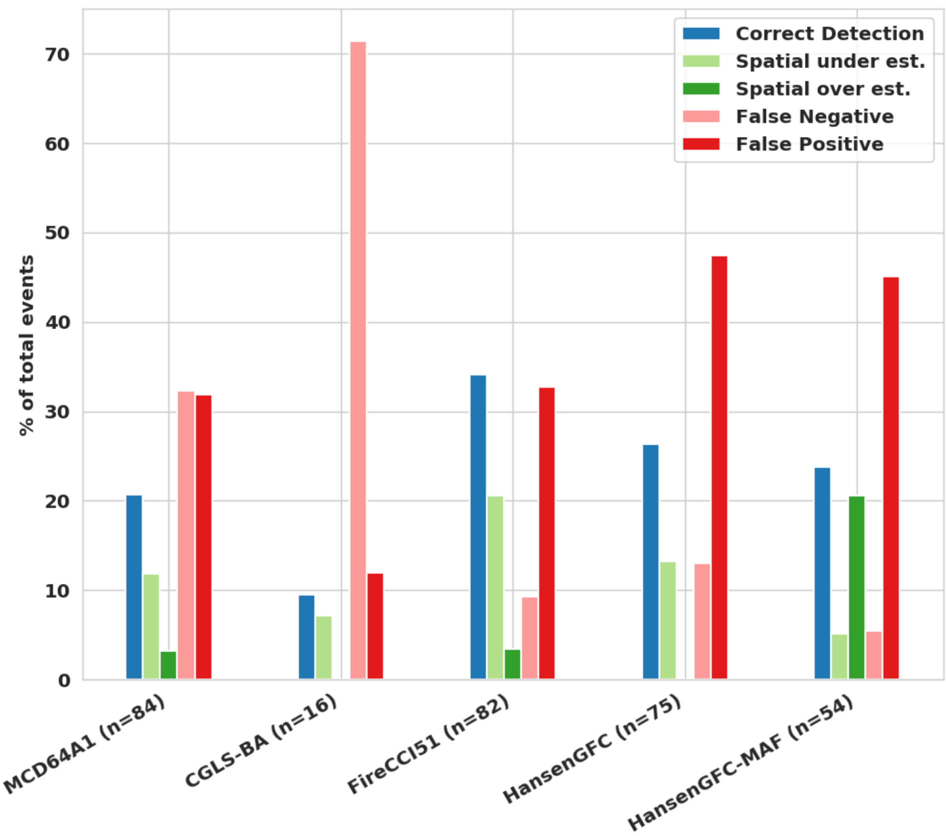

Figure 5 Accuracy of BA and forest loss products at sites in the Zabaikal region. *The BA products are compared to a manually generated fire history constructed at each site using the entire Landsat archive. An event is a burn that is observed in the Landsat record and/or the BA product.*

While the low accuracy of BA products is a problem that requires further research (Humber et al., 2019), it only impacts our ability to use FRI to infer the risk of permanent forest loss if the BA datasets have a significant positive bias (See Methods section 2.5). We find that all the BA products tend to underestimate the spatial extent of burns. MCD64A1 and CGLS-BA also have a net omission bias which suggests that the FRI's calculated using these datasets underestimate the risk of FRI-driven forest loss. While we could not assess the accuracy of GFED4 directly, it detects less burnt area in the Eurasian forest than MCD64A1. Because our results and previous studies have shown MCD64A1 to have a net omission bias (Humber et al., 2019), we therefore assume GFED4 also has a net omission bias and thereby overestimates FRI.

In contrast to MCD64A1 and CGLS-BA, the commission rate of FireCCI51 exceeds the false negative rate. Although this does suggest that the FRI calculated from FireCCI51 may overestimate the risk of permanent forest loss, our method used to assess the accuracy of the datasets is likely to overestimate the rate of False Positives (See section 2.5). The same limitation in our assessment method may also explain why HansenGFC and HansenGFC-MAF have unexpectedly high rates of commission error (Krylov et al., 2014). Previous studies have shown that MCD64A1 underestimates

BA in boreal Eurasia and that FireCCI51 corrects for this bias whilst still retaining a net omission bias (Humber et al., 2019; Lizundia-Loiola et al., 2020). Taken together, our results suggest that the FRI is a useful proxy for assessing RF risk in boreal forests and that FRI calculated using MCD64A1 and FireCCI51 are likely the most accurate, with MCD64A1 representing a lower bound on burnt area and FireCCI51 likely closest to the actual FRI.

3.3 FRI and Climatology

In the Eurasian boreal zone, previous studies have shown that FRI is strongly associated with climatology, with the shortest FRI observed in the hottest and driest parts of the boreal zone (Kharuk et al., 2021; Kharuk and Ponomarev, 2017; Ponomarev et al., 2016). Similarly, paleo reconstructions of Siberian and North American boreal fire history over the Holocene show that fire severity increases in hotter and drier periods (Feurdean et al., 2020; Gaboriau et al., 2020). Figure 6a and b show the mean annual rainfall and mean maximum monthly temperature for the period 1985 to 2015, indicating a general temperature decrease from south to north. The regions with the lowest mean annual rainfall are along the forest-steppe boundary as well as in Eastern Siberia. Broadly, this tracks with FRI estimates shown in Figure 2. Existing studies have shown that the artic-boreal region is among the fastest warming terrestrial biomes (D'Orangeville et al., 2018). The trends in annual temperature and precipitation driven by climate change are shown in Figure 6c and d, respectively, and a seasonal breakdown of the trends and the climatology are included in Supplementary Figure 2 and 3 respectively. We find that, between 1985 and 2015, climate change has driven a median increase in temperature over the Eurasian forest zone of 0.04°C per year, with most of that warming coming in winter and spring. Interestingly, while the climate change-driven trends in precipitation are mixed, only regions with negative trends are statistically significant ($\alpha_{FDR} = 0.10$). This pattern holds when considering the seasonal trends as well (Supplementary Figure 2). Over this same period, other studies have shown an increase in the frequency, extent and severity of fires throughout Siberia, which has been directly linked with climate change (Brazhnik et al., 2017; Feurdean et al., 2020; Kharuk et al., 2021; Malevsky-Malevich et al., 2008).

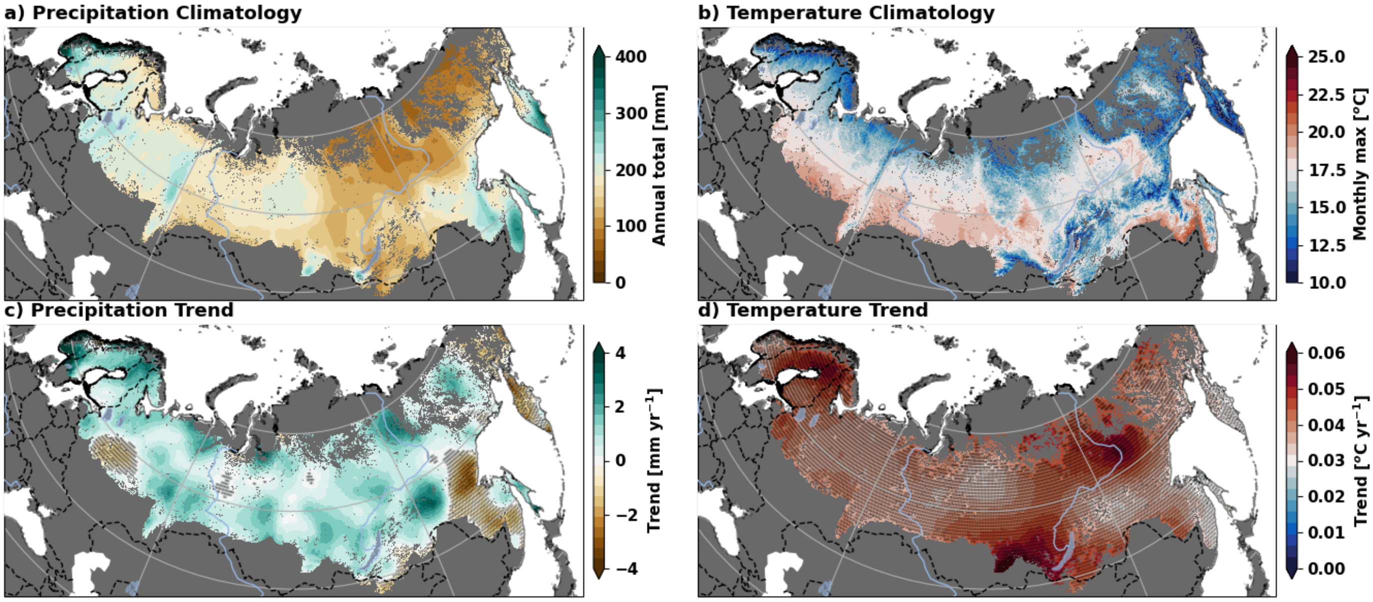

Figure 6 Climatology, climate trends and land cover. *Panels show a) the mean annual precipitation (1985 to 2015), b) the mean of the maximum monthly temperature (1985 to 2015), c) climate change-driven trend in mean annual precipitation (1985 to 2015), d) climate change-driven trend in the mean annual temperature (1985 to 2015). Non-boreal forest ecosystems are masked in grey, and, for panels c and d, the stippling indicates statistical significance (α_{FDR} = 0.10). Data: TerraClimate (Abatzoglou et al., 2018).*

To assess the link between FRI and climate quantitively, we used the machine learning method XGBoost to fit regression models between the four BA datasets and seasonal climatology with an out of sample FRI R^2 of 0.60 for GFED4, 0.54 for MCD64A1, 0.53 for CGLS-BA and 0.47 for FireCCI51. Despite having the lowest overall R^2, the FireCCI51 model has the best skill when predicting areas with FRI < 60 years and is the only model to have any skill at predicting regions with an FRI of <15 years (Figure 7a-d). All models do well in the 30 to 60, 60 to 120, and the 120 to 500 years groups but have poor performance for all FRI's > 500. Overall, we find that temperature variables have more model importance than precipitation variables, with summer temperatures being the strongest explanatory variable (Figure 7). Whilst there is generally good agreement between different models regarding feature importance, the CGLS-BA based model diverges from the other models with much lower permutation importance for winter and spring temperature. This is particularly interesting because winter and early spring climate is strongly tied to spring fire events (Feurdean et al., 2020; Kim et al., 2020), which CGLS-BA cannot detect.

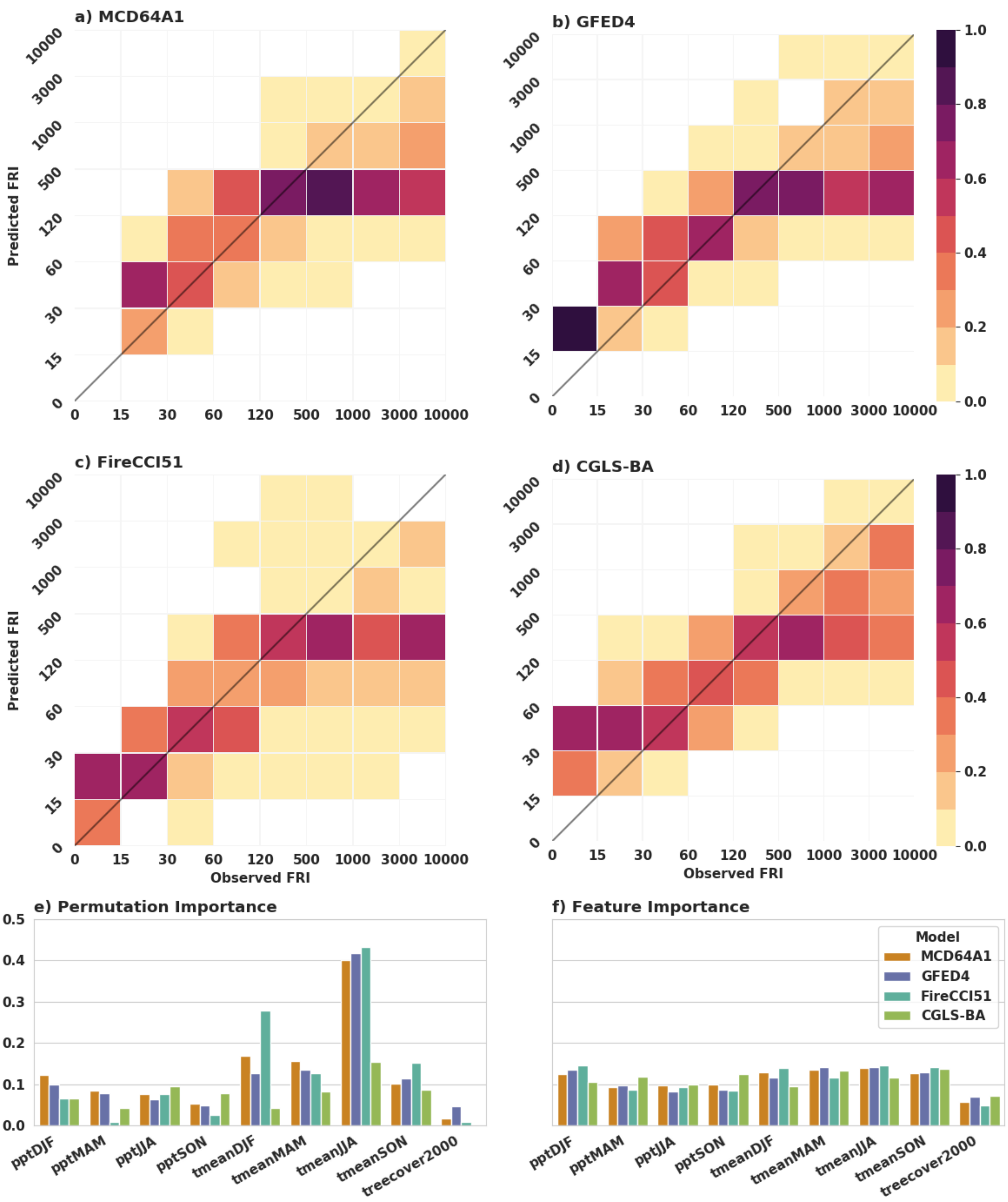

Figure 7 Modeling Landscape FRI using XGBoost. *Panels a-d show heatmaps of the observed FRI vs predicted FRI for four XGBoost models trained using a) GFED4, b) MCD64A1, c) FireCCI51, and d) CGLS-BA burnt area data. The results have been binned using the same categories as Figure 1 and then normalised by dividing the number of points in the Observed FRI category so that each column sums to 1. The black line represents the 1 to 1 line where all values would fall in a perfect model. Panels e and f show the importance of different predictor variables determined using a e) Permutation Importance*

test, and f) Feature Importance test, where ppt is mean precipitation and tmean is mean temperature for the different metorological seasons (DJF, MAM, JJA and SON) (Abatzoglou et al., 2018). treecover2000 is the fractional treecover in the year 2000 (Hansen et al., 2013).

3.4 FRI under future climate condition

To estimate how climate change may impact FRI over the next century, we used the XGBoost machine learning model fitted for the relationship between FRI and observed climatology along with four future climatology scenarios. Given current trends in climatology and the FireCCI51 model, we find that areas with a modelled FRI <30 years will increase from 0.55 M km^2 over the observed period (1985-2015) to 2.99 M km^2 by the end of the century (2085 to 2115) (Figure 8). This result also holds when our machine learning model is applied to the CMIP-5 based Terraclimate future climate dataset (TCfut) as shown in Figure 8e (2.64 M km^2 for 2085 to 2115). Both the trend and TCfut models show these increases occurring almost entirely in the coniferous forests of eastern Siberia, much of which is already at some level of permanent forest loss risk (Figure 3c). This suggests that >25 % of all Eurasian boreal forests would be at high risk of fire-driven forest loss by the end of the century. We only report the results of the FireCCI model in this section because the models derived from other datasets could not reproduce FRI <30 years over the observed period in a fully withheld testing dataset (Figure 7). The results of the other BA dataset are shown in Supplementary Figure 5-7 and the results using multivariate linear regression instead of XGBoost are shown in Supplementary Figure 8-11.

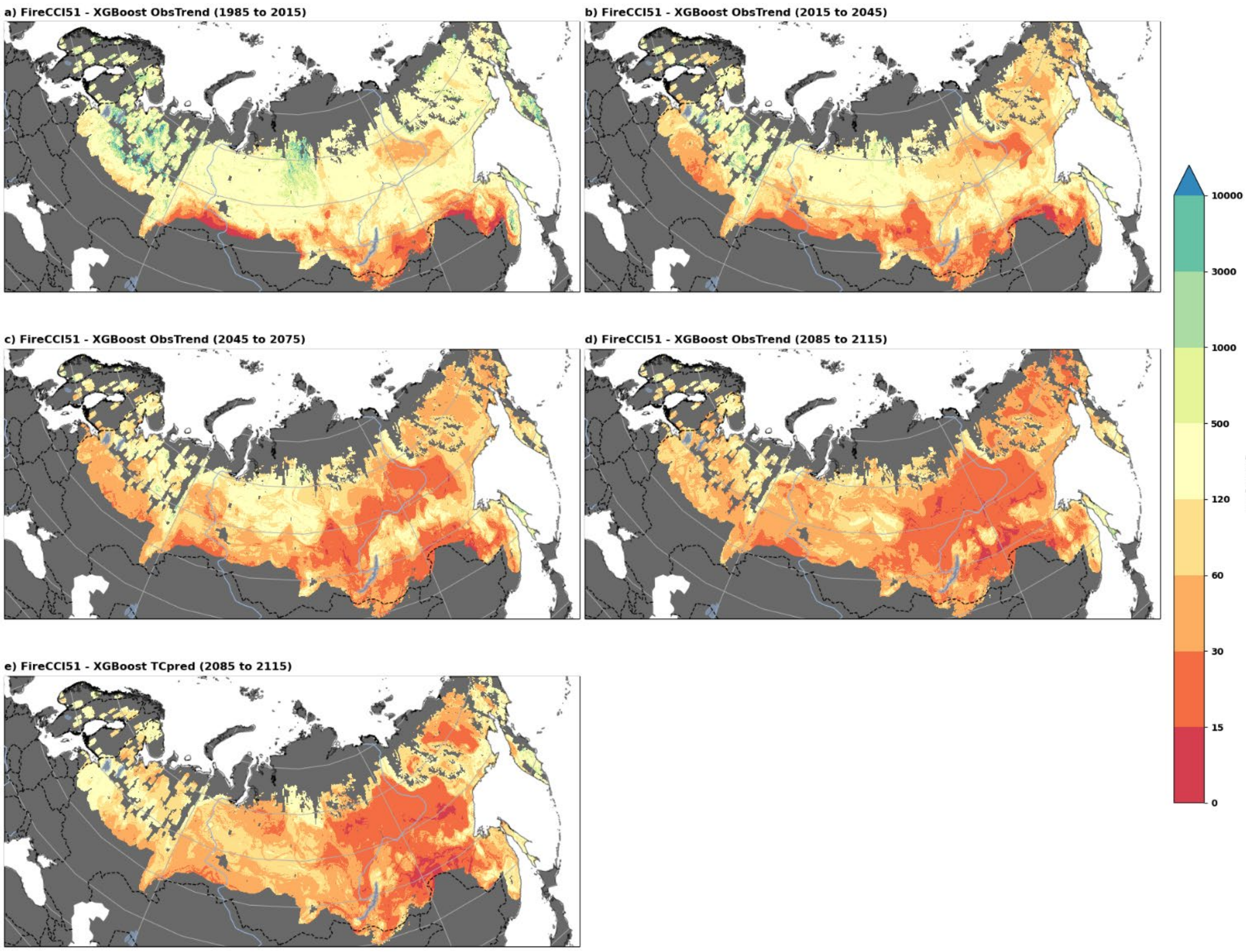

***Figure 8 Maps of the predicted FRI** a-d) based on current climate trend, XGBoost and FireCCI51 FRI data. e) TCpred is the TerraClimate prediction for a 4^{0}C warmer world, which approximates SSP3-7.0 2085 – 2115*

4. Discussion

4.1 The patterns and drivers of the observed FRI

Broadly speaking, all datasets showed a shortening of the FRI from north to south and from west to east, which is consistent with previous research and fire ecology for the region (Kharuk et al., 2021; Kharuk and Ponomarev, 2017; Ponomarev et al., 2016). However, we find higher annual burn fractions and shorter FRI's than previous studies (Kharuk et al., 2021, 2016; Ponomarev et al., 2016) likely because of inaccuracies in the BA datasets used. Both our accuracy assessment (Figure 5) and larger assessments of BA accuracy suggest that, despite significant improvements in the recent versions of the MCD64A1 and FireCCI51, all BA datasets tested have a net omission bias because BA products often fails to identify small surface fires (Humber et al., 2019; Lizundia-Loiola et al., 2020). A recent high resolution regional study in Siberia found FRI's that were far shorter than had been previously reported (Sizov et al., 2021). This suggests that even FireCCI51, the dataset with the shortest median FRI, is likely underestimating the actual annual burnt fraction.

The strong link between climatology and FRI over the Eurasian boreal zone shown in Figure 7 is consistent with previous studies that used both remotely sensed and paleo reconstructions of the fire dynamics and found that they are strongly associated with climatology (Feurdean et al., 2020; Forkel et al., 2012; Gaboriau et al., 2020; Kharuk et al., 2021; Kharuk and Ponomarev, 2017; Ponomarev et al., 2016). The summer temperature is the strongest predictor of landscape FRI (Figure 7) which is consistent with previous studies (Natole et al., 2021; Tomshin and Solovyev, 2021) and is alarming because most of eastern Eurasia is experience a summer warming rate of $>0.04^{o}C$ per year (Supplementary Figure 2). The results of this study support previous findings that hotter and drier conditions result in more frequent, and higher severity, fires (Feurdean et al., 2020; IPCC, 2021; Natole et al., 2021).

Looking at the proportion of stand replacing fires, Figure 4 shows that the likelihood of a fire being stand replacing varies considerably with dominate tree species. In the larch and pine-dominated forests of Eastern Siberia (Bartalev et al., 2004), the DRI and FRI_{SR} are extremely consistent with each other and close to 100% of fires detected are stand replacing (Figure 3c and Figure 4), which suggests that fire is the dominant driver of stand dynamics. This matches with the findings of previous studies that suggest Siberian conifer species such as *Pinus sylvestris* require a FRI_{SR} of >~150 years (Feurdean et al., 2020). The stand-replacing fire percentage in these areas is higher than would be expected considering the prevalence of low stand mortality surface fires observed in previous studies (Kharuk et al., 2021; Ponomarev et al., 2016). For example, Krylov et al., (2014) found that larch, pine and fir species have stand-replacing fire percentages in the 40 to 70% range. The discrepancy between our findings and existing studies can be explained by the BA omission bias discussed above and supports the conclusions that the BA products are omitting a large portion of the low stand mortality surface fires.

In contrast, Western Siberia, or in the Russian Far East along the Russia-China boarder north of Vladivostok, do not have a stand-replacing fire dynamic with stand-replacing fires making up <1% of BA (Figure 3c). In Western Siberia, the boreal and steppe biomes are separated by a strip of birch-dominated temperate continental forest (FAO, 2000; Feurdean et al., 2020). In these regions we find FRI_{SR} of >1000 years despite FRI's of <30 years. These findings are consistent with previous work that found short FRI's but very low stand mortality (Feurdean et al., 2020; Shuman et al., 2017) and suggest that these areas are at lower risk of permanent forest loss.

4.2 Current forest loss risk

When considered together, the FRI, FRI$_{SR}$ and the DRI can be used a proxy for the risk of permanent forest loss. Figure 9 shows the risk level and driver based on the criteria outlined in section 2.4 and Table 1. When examining the Zabaikal region, located to the east of lake Baikal near Chita in southern Siberia (Figure 6e), which is a known hotspot of post-fire recruitment failure (Barrett et al., 2020; Kukavskaya et al., 2016; Shvetsov et al., 2019), all MODIS-derived BA products have large areas with FRI's of <30 years as well as both DRI's and FRI$_{SR}$'s of <120 years. In this region the risk framework identifies large areas with high and extreme fire risk which supports the use of this framework to identify other potential hotspots.

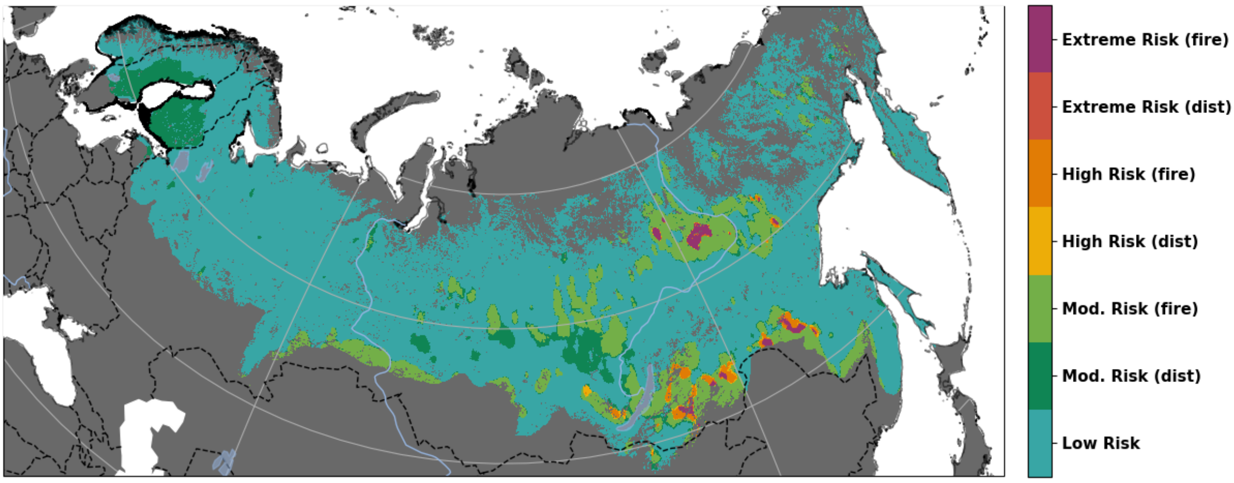

Figure 9 Current Risk of Forest Loss. *The risk of permanent forest loss using FRI, FRI$_{SR}$ and DRI over the period 2001 to 2018. Criteria are shown in Table 1*

Similar patterns to the ones found in the Zabaikal region are apparent between Krasnoyarsk and Irkutsk, as well as the forests west of Yakutsk. As such, these regions are probable hotspots of post-fire recruitment failure and forest loss. Filed based studies, most of which are published only in Russian, have found post-fire deforestation in the ribbon-like Scots pine forests grown in the zone of dry forest-steppe in the Altai region, Minusinsk stands of the Krasnoyarsk krai, Balgazynsky pine forests of the Tyva Republic (Buryak et al., 2011; Ishutin, 2004; Kupriyanov et al., 2003; Paramonov and Ishutin, 1999) (Buryak et al., 2011; Ishutin, 2004; Kupriyanov et al., 2009; Paramonov, Ishutin, 1999). At time of writing, the authors of this study are away of no studies looking at postfire RF in Yakutia and the Far East. In total there are 133,235 km^2 of forests that are at high or extreme risk of fire driven permanent forest loss (Figure 3c).

In the Zabaikal and Yakutia regions, the risk framework shown in Figure 9 identified high or extreme disturbance-driven risk. The link between DRI and permanent forest loss is more nuanced than the link with FRI. When a short DRI is coincident with a short FRI, it can drive forest loss by increasing the *"resilience debt"* (Burrell et al., 2021; Johnstone et al., 2016). Previous studies have shown that repeat disturbances, especially post-fire salvage logging which is a common practice in many regions, contributes to recruitment failure in Siberia (Burrell et al., 2021; Kukavskaya et al., 2016). Logging can also replace the initial stand-replacing fire in the RF regime. In Russia, it is standard practice to replant trees after logging, but ~50% of the areas replanted in the most fire-prone parts of southern Siberia burn again within 15 years (Kukavskaya et al., 2016), which is likely to result in RF and forest loss. By contrast, in Scandinavia, where there is a <120 year DRI as the result of the widespread managed forestry (Curtis et al., 2018; Hansen et al., 2013) but a FRI of > 10,000 years, there is likely low risk of permanent forest loss. Interestingly, DRI's over central and western Eurasia are considerably shorter than the FRI_{SR}, which indicates forest loss is still prevalent, even if it is not being caused by fires (Figure 3b) (Curtis et al., 2018). Given this nuanced relationship, areas with a short FRI and short DRI's, but much longer FRI_{SR} (Mod. Risk and High Risk (dist) in Figure 3c), are arguably still at higher risk of forest loss and should be the focus of future research.

4.3 Future forest loss risk

Our modelling results predict that the region will experience a large and consistent increase in the area with a predicted FRI <30 years throughout the next century as the earth warms (Figure 8). Applying the risk criteria detailed in Table 1 and shown in Figure 9 to the predictions of FRI shown in Figure 8, we estimate that 530, 000 km^2 is at high or extreme risk of fire-induced forest loss during the2015 to 2045 window, almost double the amount of area predicted for the 1985-2015 reference period. Both the 2020 and 2021 fire seasons, which are not included in the data used in this study, have been exceptionally large with some of the largest burns occurring in Yakutia (Ponomarev et al., 2021).

Looking out to the end of the century, both the trend-based and CMIP model-based estimates of future risk predict more than 2.5M km^2 (>20%) will have high or extreme risk of forest loss, with almost all of this increase in the risk of future fire-driven forest loss occurring over the pine and larch forests of Eastern Eurasia. Figure 10 shows the predicted forest risk loss using the current trends in climatology.

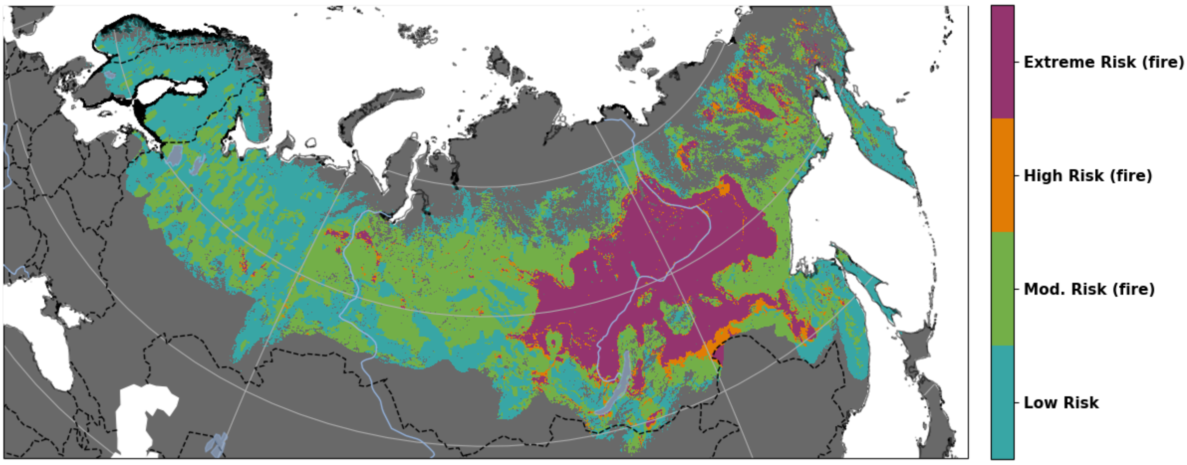

Figure 10 Risk of Forest Loss by 2085 to 2115. *The risk of permanent forest loss using future FRI estimated using XGBoost and FireCCI51, assuming that the fraction of fires that are stand-replacing remains constant through time. Criteria are shown in Table 1.*

Current Earth System Models, Land Surface Models, and even ecosystem-scale forest models, predict or assume gains or stability in the extent of boreal tree cover (Friend et al., 2014; Shuman et al., 2017). These models often underestimate the FRI (Shuman et al., 2017) if they include disturbance at all, and do not consider the possibility of fire-induced forest loss. Currently, the best prediction of ecosystem change in the Eurasian boreal zone use Species Distribution Models (SDMs) in combination with Earth System Models (ESM) to investigate changes in habitat suitability (Noce et al., 2019). This modelling approach predicts significant changes in the dominant species across Eurasia, but no major shift in the extent of forest zone itself. However, this approach does not consider fire and cannot account for post-fire RF (Noce et al., 2019). The most recent IPCC report identified uncertainties around indirect CO_2 emissions from things like forest fires as a key limitation that can greatly impact our ability to predict the changes that will occur over the next 100 years (IPCC, 2021).

Eastern Eurasia contains some of the largest areas of unmanaged primary forest in the world (Potapov et al., 2017) and the widespread loss of forest in this region will accelerate the loss of habitats and associated biodiversity that is already occurring at an alarming rate (Brondizio et al., 2019; Dinerstein et al., 2017). Siberia contains globally significant amounts of stored carbon in both the above ground biomass and the soil (Brondizio et al., 2019; Kharuk et al., 2021). Previous studies have shown than increases in the frequency of fires will drive widespread carbon loss and amplify the impacts of climate change (de Groot et al., 2013; Kharuk et al., 2021). In addition to the global impacts, an increase in fire frequency will likely worsen the air quality problems and associated health issues that already occur in cities like Novosibirsk, Krasnoyarsk and Yakutsk during large fire years (Kharuk et al., 2021). The loss of forest goods and commercially valuable tree species is likely to negatively impact upon the economic and social well-being of the local population which are reliant on the forestry industry (Leskinen et al., 2020) and could contribute to the further loss of indigenous culture and language in the region (Brondizio et al., 2019).

4.4 The limitations of future predictions of forest loss

The main limitation of our FRI prediction approach is that we are unable to consider secondary effects and feedback loops. For example, the increased burning may have a long-term negative feedback on fire frequency because of reductions in fuel availability (Bernier et al., 2016). Nevertheless, increases in drought severity and summer temperatures may lead to a large increase in the portion of fires that are stand-replacing (de Groot et al., 2013; Tepley et al., 2018). At the same time, heatwave and drought events which are increasing with climate change and potentially greatly reducing the survivability of seedling and saplings (Boucher et al., 2019; Sannikov et al., 2020). Our modelling approach assumes a constant tree cover, but there is strong evidence that forest fragmentation directly increases the frequency of fires (Tepley et al., 2018).

One feedback loop that might act to mitigate the risk of fire induced forest loss is the species balance shift from conifers to broadleaf tree species such as Aspen (*Populus tremuloides*) (Gill et al., 2017; Johnstone and Chapin, 2006; Whitman et al., 2019). This transition has been widely observed in boreal North America (Gill et al., 2017; Johnstone and Chapin, 2006; Whitman et al., 2019), and has been described as a potential strategy to mitigate the impact of increase in forest fires (Astrup et al., 2018). Whilst this dynamic has also been observed in Eurasia (Kharuk et al., 2021), it is highly unlikely to be able to offset the forest loss predicted by this study. In Eurasia, temperature, and to a lesser extent, water availability, is the key limiting factor in reshaping species ranges and whilst models currently predict a significant expansion in the range of Aspen throughout this century (Noce et al., 2019), almost all this expansion is predicted to occur in western Eurasia, with almost none occurring in areas where we predict fire-induced forest loss risk increases.

When the potential increase in stand-replacing fires, the reduced survivability of seedlings and the increase in fire frequency are considered together, it points to a strong likelihood of a positive feedback mechanism which, in turn, raises the concerning possibility that the predictions shown in Figure 8 may actually underestimate the risk of future FRI induced forest loss. Unlike boreal North America, species balance shifts are much less likely to mitigate the risk of increased fires.

5. Conclusions

Characterizing the changing extent of the boreal forest biome is essential for understanding the impacts of climate change on the biosphere and feedbacks to future climate change (Kharuk et al., 2021). Our results show that 1.2 % of the Eurasian boreal zone is already at high or extreme risk of fire induced forest loss with a further 11 % of areas at moderate risk. Given current warming rates, >20 % of the Eurasian forest zone is likely to be at high risk by the end of the century. This poses a substantial risk to the forestry industry in the region and has the potential to dampen, and potentially, even reverse, the boreal carbon sink. As such, there is an urgent need for more research to examine this critical dynamic in the field and to include it in models of vegetation and climate feedbacks.

6. Acknowledgments

This work was supported by (i) the UK Natural Environment Research Council [grant number NE/N009495/1] awarded to KB and RB and (ii) the National Aeronautics and Space Administration (NASA) Arctic Boreal Vulnerability Experiment (ABoVE) grant 80NSSC19M0112. EK and SZ acknowledge funding support from the RFBR, Government of the Krasnoyarsk krai and the Krasnoyarsk regional foundation of scientific and scientific-technical support (Grant #20-44-242004).

7. Author contributions

ALB and KB conceived the study. ALB developed the methodology with input from KB, RB and QS. ALB performed the analysis and wrote the manuscript with input from QS, RB, EAK, SZ, TS, BMR and KB.

8. Data Availability

All datasets used in this study are publicly available and can be accessed from their original creators.

9. Code availability

The code is available by request to the corresponding author.

10. References

Abatzoglou, J.T., Dobrowski, S.Z., Parks, S.A., Hegewisch, K.C., 2018. TerraClimate, a high-resolution global dataset of monthly climate and climatic water balance from 1958–2015. Sci. Data 5, 170191. https://doi.org/10.1038/sdata.2017.191

Archibald, S., Lehmann, C.E.R., Gómez-Dans, J.L., Bradstock, R.A., 2013. Defining pyromes and global syndromes of fire regimes. Proc. Natl. Acad. Sci. 201211466. https://doi.org/10.1073/pnas.1211466110

Astrup, R., Bernier, P.Y., Genet, H., Lutz, D.A., Bright, R.M., 2018. A sensible climate solution for the boreal forest. Nat. Clim. Change 8, 11–12. https://doi.org/10.1038/s41558-017-0043-3

Baltzer, J.L., Day, N.J., Walker, X.J., Greene, D.F., Mack, M.C., Alexander, H.D., Arseneault, D., Barnes, J.L., Bergeron, Y., Boucher, Y., Bourgeau-Chavez, L., Brown, C.D., Carrière, S., Howard, B., Gauthier, S., Parisien, M.-A., Reid, K.A., Rogers, B.M., Roland, C.A., Sirois, L., Stehn, S.E., Thompson, D.K., Turetsky, M.R., Veraverbeke, S., Whitman, E., Yang, J., Johnstone, J.F., In Press. From resilience to regeneration failure: is black spruce at a tipping point in boreal North America? Proc. Natl. Acad. Sci.

Barrett, K., Baxter, R., Kukavskaya, E., Balzter, H., Shvetsov, E., Buryak, L., 2020. Postfire recruitment failure in Scots pine forests of southern Siberia. Remote Sens. Environ. 237, 111539. https://doi.org/10.1016/j.rse.2019.111539

Bartalev, S., Yaroshenko, A., Ershov, D., A.S., I., Potapov, P., Turubanova, S., 2004. Russia’s Forests Dominating Forest Types and Their Canopy Density.

Bartholomé, E., Belward, A.S., 2005. GLC2000: a new approach to global land cover mapping from Earth observation data. Int. J. Remote Sens. 26, 1959–1977. https://doi.org/10.1080/01431160412331291297

Bernier, P.Y., Gauthier, S., Jean, P.-O., Manka, F., Boulanger, Y., Beaudoin, A., Guindon, L., 2016. Mapping Local Effects of Forest Properties on Fire Risk across Canada. Forests 7, 157. https://doi.org/10.3390/f7080157

Beverly, J.L., Beverly, J.L., 2017. Time since prior wildfire affects subsequent fire containment in black spruce. Int. J. Wildland Fire 26, 919–929. https://doi.org/10.1071/WF17051

Boucher, D., Gauthier, S., Thiffault, N., Marchand, W., Girardin, M., Urli, M., 2019. How climate change might affect tree regeneration following fire at northern latitudes: a review. New For. https://doi.org/10.1007/s11056-019-09745-6

Bradshaw, C.J.A., Warkentin, I.G., 2015. Global estimates of boreal forest carbon stocks and flux. Glob. Planet. Change 128, 24–30. https://doi.org/10.1016/j.gloplacha.2015.02.004

Brazhnik, K., Hanley, C., Shugart, H.H., 2017. Simulating Changes in Fires and Ecology of the 21st Century Eurasian Boreal Forests of Siberia. Forests 8, 49. https://doi.org/10.3390/f8020049

Brennan, J., Gómez-Dans, J.L., Disney, M., Lewis, P., 2019. Theoretical uncertainties for global satellite-derived burned area estimates. Biogeosciences 16, 3147–3164. https://doi.org/10.5194/bg-16-3147-2019

Brodie, J.F., Roland, C.A., Stehn, S.E., Smirnova, E., 2019. Variability in the expansion of trees and shrubs in boreal Alaska. Ecology e02660. https://doi.org/10.1002/ecy.2660

Brondizio, E.S., Settele, J., Díaz, S., Ngo, H.T., 2019. Global assessment report on biodiversity and ecosystem services of the Intergovernmental Science-Policy Platform on Biodiversity and Ecosystem Services. IPBES Secr. Bonn.

Broome, A., Summers, R.W., Vanhala, T., 2016. Understanding the provision of conifer seed for woodland species. Res. Note-For. Comm.

Brown, C.D., Johnstone, J.F., 2012. Once burned, twice shy: Repeat fires reduce seed availability and alter substrate constraints on Picea mariana regeneration. For. Ecol. Manag. 266, 34–41. https://doi.org/10.1016/j.foreco.2011.11.006

Burrell, A.L., Evans, J.P., De Kauwe, M.G., 2020. Anthropogenic climate change has driven over 5 million km 2 of drylands towards desertification. Nat. Commun. 11, 3853. https://doi.org/10.1038/s41467-020-17710-7

Burrell, A.L., Evans, J.P., Liu, Y., 2019. The Addition of Temperature to the TSS-RESTREND Methodology Significantly Improves the Detection of Dryland Degradation. IEEE J. Sel. Top. Appl. Earth Obs. Remote Sens. 1–7. https://doi.org/10.1109/JSTARS.2019.2906466

Burrell, A.L., Kukavskaya, E.A., Baxter, R., Sun, Q., Barrett, K., 2021. Post-fire recruitment failure as a driver of forest to non-forest ecosystem shifts in boreal regions, in: Ecosystem Collapse and Climate Change, Ecological Studies. Springer International Publishing.

Buryak, L.V., Sukhinin, A.I., Kalenskaya, O.P., Ponomarev, E.I., 2011. Effects of fires in ribbon-like pine forests of southern Siberia. Contemp. Probl. Ecol. 4, 248–253. https://doi.org/10.1134/S1995425511030039

Cai, W.H., Liu, Z., Yang, Y.Z., Yang, J., 2018. Does Environment Filtering or Seed Limitation Determine Post-fire Forest Recovery Patterns in Boreal Larch Forests? Front. Plant Sci. 9. https://doi.org/10.3389/fpls.2018.01318

CDO, 2018. Climate Data Operators.

Chen, D., Loboda, T.V., 2018. Surface forcing of non-stand-replacing fires in Siberian larch forests. Environ. Res. Lett. 13, 045008. https://doi.org/10.1088/1748-9326/aab443

Chen, H.Y.H., Luo, Y., Reich, P.B., Searle, E.B., Biswas, S.R., 2016. Climate change-associated trends in net biomass change are age dependent in western boreal forests of Canada. Ecol. Lett. 19, 1150–1158. https://doi.org/10.1111/ele.12653

Chen, T., Guestrin, C., 2016. XGBoost: A Scalable Tree Boosting System. Proc. 22nd ACM SIGKDD Int. Conf. Knowl. Discov. Data Min. 785–794. https://doi.org/10.1145/2939672.2939785

Chmura, D.J., Rożkowski, R., Chałupka, W., 2012. Growth and phenology variation in progeny of Scots pine seed orchards and commercial seed stands. Eur. J. For. Res. 131, 1229–1243. https://doi.org/10.1007/s10342-012-0594-9

Chu, T., Guo, X., 2014. Remote Sensing Techniques in Monitoring Post-Fire Effects and Patterns of Forest Recovery in Boreal Forest Regions: A Review. Remote Sens. 6, 470–520. https://doi.org/10.3390/rs6010470

Coops, N.C., Hermosilla, T., Wulder, M.A., White, J.C., Bolton, D.K., 2018. A thirty year, fine-scale, characterization of area burned in Canadian forests shows evidence of regionally increasing trends in the last decade. PLOS ONE 13, e0197218. https://doi.org/10.1371/journal.pone.0197218

Curtis, P.G., Slay, C.M., Harris, N.L., Tyukavina, A., Hansen, M.C., 2018. Classifying drivers of global forest loss. Science 361, 1108–1111. https://doi.org/10.1126/science.aau3445

de Groot, W.J., Cantin, A.S., Flannigan, M.D., Soja, A.J., Gowman, L.M., Newbery, A., 2013. A comparison of Canadian and Russian boreal forest fire regimes. For. Ecol. Manag., The Mega-fire reality 294, 23–34. https://doi.org/10.1016/j.foreco.2012.07.033

Dinerstein, E., Olson, D., Joshi, A., Vynne, C., Burgess, N.D., Wikramanayake, E., Hahn, N., Palminteri, S., Hedao, P., Noss, R., Hansen, M., Locke, H., Ellis, E.C., Jones, B., Barber, C.V., Hayes, R., Kormos, C., Martin, V., Crist, E., Sechrest, W., Price, L., Baillie, J.E.M., Weeden, D., Suckling, K., Davis, C., Sizer, N., Moore, R., Thau, D., Birch, T., Potapov, P., Turubanova, S., Tyukavina, A., de Souza, N., Pintea, L., Brito, J.C., Llewellyn, O.A., Miller, A.G., Patzelt, A., Ghazanfar, S.A., Timberlake, J., Klöser, H., Shennan-Farpón, Y., Kindt, R., Lillesø, J.-P.B., van Breugel, P., Graudal, L., Voge, M., Al-Shammari, K.F., Saleem, M., 2017. An Ecoregion-Based Approach to Protecting Half the Terrestrial Realm. BioScience 67, 534–545. https://doi.org/10.1093/biosci/bix014

D’Orangeville, L., Houle, D., Duchesne, L., Phillips, R.P., Bergeron, Y., Kneeshaw, D., 2018. Beneficial effects of climate warming on boreal tree growth may be transitory. Nat. Commun. 9, 3213. https://doi.org/10.1038/s41467-018-05705-4

Erni, S., Arseneault, D., Parisien, M.-A., 2018. Stand Age Influence on Potential Wildfire Ignition and Spread in the Boreal Forest of Northeastern Canada. Ecosystems 21, 1471–1486. https://doi.org/10.1007/s10021-018-0235-3

Falk, D.A., Miller, C., McKenzie, D., Black, A.E., 2007. Cross-Scale Analysis of Fire Regimes. Ecosystems 10, 809–823. https://doi.org/10.1007/s10021-007-9070-7

FAO, 2000. Global Forest Resources Assessment 2000: Main Reports (FAO Forestry Paper No. 140). UN Food and Agriculture Organization, Rome.

Feurdean, A., Florescu, G., Tanţău, I., Vannière, B., Diaconu, A.-C., Pfeiffer, M., Warren, D., Hutchinson, S.M., Gorina, N., Gałka, M., Kirpotin, S., 2020. Recent fire regime in the southern boreal forests of western Siberia is unprecedented in the last five millennia. Quat. Sci. Rev. 244, 106495. https://doi.org/10.1016/j.quascirev.2020.106495

Forbes, B.C., Fauria, M.M., Zetterberg, P., 2010. Russian Arctic warming and ‘greening’ are closely tracked by tundra shrub willows. Glob. Change Biol. 16, 1542–1554. https://doi.org/10.1111/j.1365-2486.2009.02047.x

Forkel, M., Thonicke, K., Beer, C., Cramer, W., Bartalev, S., Schmullius, C., 2012. Extreme fire events are related to previous-year surface moisture conditions in permafrost-underlain larch forests of Siberia. Environ. Res. Lett. 7, 044021. https://doi.org/10.1088/1748-9326/7/4/044021

Frazier, R.J., Coops, N.C., Wulder, M.A., Hermosilla, T., White, J.C., 2018. Analyzing spatial and temporal variability in short-term rates of post-fire vegetation return from Landsat time series. Remote Sens. Environ. 205, 32–45. https://doi.org/10.1016/j.rse.2017.11.007

Friend, A.D., Lucht, W., Rademacher, T.T., Keribin, R., Betts, R., Cadule, P., Ciais, P., Clark, D.B., Dankers, R., Falloon, P.D., Ito, A., Kahana, R., Kleidon, A., Lomas, M.R., Nishina, K., Ostberg, S., Pavlick, R., Peylin, P., Schaphoff, S., Vuichard, N., Warszawski, L., Wiltshire, A., Woodward, F.I., 2014. Carbon residence time dominates uncertainty in terrestrial vegetation responses to future climate and atmospheric CO2. Proc. Natl. Acad. Sci. 111, 3280–3285. https://doi.org/10.1073/pnas.1222477110

Gaboriau, D.M., Remy, C.C., Girardin, M.P., Asselin, H., Hély, C., Bergeron, Y., Ali, A.A., 2020. Temperature and fuel availability control fire size/severity in the boreal forest of central Northwest Territories, Canada. Quat. Sci. Rev. 250, 106697. https://doi.org/10.1016/j.quascirev.2020.106697

Gauthier, S., Bernier, P., Kuuluvainen, T., Shvidenko, A.Z., Schepaschenko, D.G., 2015. Boreal forest health and global change. Science 349, 819–822. https://doi.org/10.1126/science.aaa9092

Giglio, L., Boschetti, L., Roy, D.P., Humber, M.L., Justice, C.O., 2018. The Collection 6 MODIS burned area mapping algorithm and product. Remote Sens. Environ. 217, 72–85. https://doi.org/10.1016/j.rse.2018.08.005

Gill, N.S., Sangermano, F., Buma, B., Kulakowski, D., 2017. Populus tremuloides seedling establishment: An underexplored vector for forest type conversion after multiple disturbances. For. Ecol. Manag. 404, 156–164. https://doi.org/10.1016/j.foreco.2017.08.008

Goetz, S.J., Bunn, A.G., Fiske, G.J., Houghton, R.A., 2005. Satellite-observed photosynthetic trends across boreal North America associated with climate and fire disturbance. Proc. Natl. Acad. Sci. 102, 13521–13525. https://doi.org/10.1073/pnas.0506179102

Goetz, S.J., Miller, C.E., Griffith, P., Chatterjee, A., Boelman, N., Bourgeau-Chavez, L., Butman, D., Epstein, H.E., Fisher, J.B., French, N.H.F., Hoy, E., Kimball, J.S., Larson, E., Loboda, T., Mack, M.C., Moghaddam, M., Montesano, P.M., Prugh, L., Rawlins, M., Rocha, A.V., Rogers, B.M., Schaefer, K., In Review. An overview of NASA’s Arctic Boreal Vulnerability Experiment (ABoVE): Development, implementation, advances and knowledge gaps.

Guay, K.C., Beck, P.S.A., Berner, L.T., Goetz, S.J., Baccini, A., Buermann, W., 2014. Vegetation productivity patterns at high northern latitudes: a multi-sensor satellite data assessment. Glob. Change Biol. 20, 3147–3158. https://doi.org/10.1111/gcb.12647

Hansen, M.C., Potapov, P.V., Moore, R., Hancher, M., Turubanova, S.A., Tyukavina, A., Thau, D., Stehman, S.V., Goetz, S.J., Loveland, T.R., Kommareddy, A., Egorov, A., Chini, L., Justice, C.O., Townshend, J.R.G., 2013. High-Resolution Global Maps of 21st-Century Forest Cover Change. Science 342, 850–853. https://doi.org/10.1126/science.1244693

Hansen, W.D., Braziunas, K.H., Rammer, W., Seidl, R., Turner, M.G., 2018. It takes a few to tango: changing climate and fire regimes can cause regeneration failure of two subalpine conifers. Ecology 99, 966–977. https://doi.org/10.1002/ecy.2181

Hayasaka, H., Sokolova, G.V., Ostroukhov, A., Naito, D., 2020. Classification of Active Fires and Weather Conditions in the Lower Amur River Basin. Remote Sens. 12, 3204. https://doi.org/10.3390/rs12193204

Hayes, D.J., McGuire, A.D., Kicklighter, D.W., Gurney, K.R., Burnside, T.J., Melillo, J.M., 2011. Is the northern high-latitude land-based CO2 sink weakening? Glob. Biogeochem. Cycles 25. https://doi.org/10.1029/2010GB003813

Huang, J., Tardif, J.C., Bergeron, Y., Denneler, B., Berninger, F., Girardin, M.P., 2010. Radial growth response of four dominant boreal tree species to climate along a latitudinal gradient in the eastern Canadian boreal forest. Glob. Change Biol. 16, 711–731. https://doi.org/10.1111/j.1365-2486.2009.01990.x

Humber, M.L., Boschetti, L., Giglio, L., Justice, C.O., 2019. Spatial and temporal intercomparison of four global burned area products. Int. J. Digit. Earth 12, 460–484. https://doi.org/10.1080/17538947.2018.1433727

IPCC, 2021. Climate Change 2021: The Physical Science Basis. Contribution of Working Group I to the Sixth Assessment Report of the Intergovernmental Panel on Climate Change.

Ishutin, Ya.N., 2004. Reforestation of Burned Areas in Ribbon-Like Pine Forest of Altai (Barnaul, 2004) [in Russian].

Johnstone, J.F., Allen, C.D., Franklin, J.F., Frelich, L.E., Harvey, B.J., Higuera, P.E., Mack, M.C., Meentemeyer, R.K., Metz, M.R., Perry, G.L., Schoennagel, T., Turner, M.G., 2016. Changing disturbance regimes, ecological memory, and forest resilience. Front. Ecol. Environ. 14, 369–378. https://doi.org/10.1002/fee.1311

Johnstone, J.F., Chapin, F.S., 2006. Effects of Soil Burn Severity on Post-Fire Tree Recruitment in Boreal Forest. Ecosystems 9, 14–31. https://doi.org/10.1007/s10021-004-0042-x

Johnstone, J.F., Hollingsworth, T.N., Chapin, F.S., Mack, M.C., 2010. Changes in fire regime break the legacy lock on successional trajectories in Alaskan boreal forest. Glob. Change Biol. 16, 1281–1295. https://doi.org/10.1111/j.1365-2486.2009.02051.x

Kauppi, P.E., Posch, M., Pirinen, P., 2014. Large Impacts of Climatic Warming on Growth of Boreal Forests since 1960. PLOS ONE 9, e111340. https://doi.org/10.1371/journal.pone.0111340

Keenan, T.F., Riley, W.J., 2018. Greening of the land surface in the world’s cold regions consistent with recent warming. Nat. Clim. Change 1. https://doi.org/10.1038/s41558-018-0258-y

Kharuk, V.I., Dvinskaya, M.L., Petrov, I.A., Im, S.T., Ranson, K.J., 2016. Larch forests of Middle Siberia: long-term trends in fire return intervals. Reg. Environ. Change 16, 2389–2397. https://doi.org/10.1007/s10113-016-0964-9

Kharuk, V.I., Ponomarev, E.I., 2017. Spatiotemporal characteristics of wildfire frequency and relative area burned in larch-dominated forests of Central Siberia. Russ. J. Ecol. 48, 507–512. https://doi.org/10.1134/S1067413617060042

Kharuk, V.I., Ponomarev, E.I., Ivanova, G.A., Dvinskaya, M.L., Coogan, S.C.P., Flannigan, M.D., 2021. Wildfires in the Siberian taiga. Ambio. https://doi.org/10.1007/s13280-020-01490-x

Kim, J.-S., Kug, J.-S., Jeong, S.-J., Park, H., Schaepman-Strub, G., 2020. Extensive fires in southeastern Siberian permafrost linked to preceding Arctic Oscillation. Sci. Adv. 6, eaax3308. https://doi.org/10.1126/sciadv.aax3308

Koven, C.D., 2013. Boreal carbon loss due to poleward shift in low-carbon ecosystems. Nat. Geosci. 6, 452–456. https://doi.org/10.1038/ngeo1801

Krylov, A., McCarty, J.L., Potapov, P., Loboda, T., Tyukavina, A., Turubanova, S., Hansen, M.C., 2014. Remote sensing estimates of stand-replacement fires in Russia, 2002–2011. Environ. Res. Lett. 9, 105007. https://doi.org/10.1088/1748-9326/9/10/105007

Kukavskaya, E.A., Buryak, L.V., Shvetsov, E.G., Conard, S.G., Kalenskaya, O.P., 2016. The impact of increasing fire frequency on forest transformations in southern Siberia. For. Ecol. Manag. 382, 225–235. https://doi.org/10.1016/j.foreco.2016.10.015

Kukavskaya, E.A., Ivanova, G.A., Conard, S.G., McRae, D.J., Ivanov, V.A., 2014. Biomass dynamics of central Siberian Scots pine forests following surface fires of varying severity. Int. J. Wildland Fire 23, 872–886. https://doi.org/10.1071/WF13043

Kupriyanov, A.N., Trofimov, I.T., Zablotskiy, V.I., Makarychev, S.V., Kudryashov, I.V., Malinovskikh, A.A., Burmistrov, M.V., Strakowski, A.N., Bolotov, A.G., Begovich, Y., 2003. Restoration of forest ecosystems after fires.

Leskinen, P., Lindner, M., Verkerk, P.J., Nabuurs, G.-J., Van Brusselen, J., Kulikova, E., Hassegawa, M., Lerink, B. (Eds.), 2020. Russian forests and climate change, What Science Can Tell Us. European Forest Institute. https://doi.org/10.36333/wsctu11

Lin, X., Rogers, B.M., Sweeney, C., Chevallier, F., Arshinov, M., Dlugokencky, E., Machida, T., Sasakawa, M., Tans, P., Keppel-Aleks, G., 2020. Siberian and temperate ecosystems shape Northern Hemisphere atmospheric CO2 seasonal amplification. Proc. Natl. Acad. Sci. 117, 21079–21087. https://doi.org/10.1073/pnas.1914135117

Linder, P., Jonsson, P., Niklasson, M., 1998. Tree mortality after prescribed burning in an old-growth Scots pine forest in northern Sweden. Silva Fenn. 32. https://doi.org/10.14214/sf.675

Liu, Y.Y., Dijk, A.I.J.M. van, Jeu, R.A.M. de, Canadell, J.G., McCabe, M.F., Evans, J.P., Wang, G., 2015. Recent reversal in loss of global terrestrial biomass. Nat. Clim. Change 5, 470–474. https://doi.org/10.1038/nclimate2581

Lizundia-Loiola, J., Otón, G., Ramo, R., Chuvieco, E., 2020. A spatio-temporal active-fire clustering approach for global burned area mapping at 250 m from MODIS data. Remote Sens. Environ. 236, 111493. https://doi.org/10.1016/j.rse.2019.111493

Malevsky-Malevich, S.P., Molkentin, E.K., Nadyozhina, E.D., Shklyarevich, O.B., 2008. An assessment of potential change in wildfire activity in the Russian boreal forest zone induced by climate warming during the twenty-first century. Clim. Change 86, 463–474. https://doi.org/10.1007/s10584-007-9295-7

Myers-Smith, I.H., Forbes, B.C., Wilmking, M., Hallinger, M., Lantz, T., Blok, D., Tape, K.D., Macias-Fauria, M., Sass-Klaassen, U., Lévesque, E., Boudreau, S., Ropars, P., Hermanutz, L., Trant, A., Collier, L.S., Weijers, S., Rozema, J., Rayback, S.A., Schmidt, N.M., Schaepman-Strub, G., Wipf, S., Rixen, C., Ménard, C.B., Venn, S., Goetz, S., Andreu-Hayles, L., Elmendorf, S., Ravolainen, V., Welker, J., Grogan, P., Epstein, H.E., Hik, D.S., 2011. Shrub expansion in tundra ecosystems: dynamics, impacts and research priorities. Environ. Res. Lett. 6, 045509. https://doi.org/10.1088/1748-9326/6/4/045509

Natole, M., Ying, Y., Buyantuev, A., Stessin, M., Buyantuev, V., Lapenis, A., 2021. Patterns of mega-forest fires in east Siberia will become less predictable with climate warming. Environ. Adv. 4, 100041. https://doi.org/10.1016/j.envadv.2021.100041

Noce, S., Caporaso, L., Santini, M., 2019. Climate Change and Geographic Ranges: The Implications for Russian Forests. Front. Ecol. Evol. 7, 57. https://doi.org/10.3389/fevo.2019.00057

Pan, Y., Birdsey, R.A., Fang, J., Houghton, R., Kauppi, P.E., Kurz, W.A., Phillips, O.L., Shvidenko, A., Lewis, S.L., Canadell, J.G., Ciais, P., Jackson, R.B., Pacala, S.W., McGuire, A.D., Piao, S., Rautiainen, A., Sitch, S., Hayes, D., 2011. A Large and Persistent Carbon Sink in the World's Forests. Science 333, 988–993. https://doi.org/10.1126/science.1201609

Paramonov, E.G., Ishutin, Ya.N., 1999. Large Fires in Altai Krai (Barnaul, 1999) [in Russian].

Payette, S., Delwaide, A., 2003. Shift of Conifer Boreal Forest to Lichen–Heath Parkland Caused by Successive Stand Disturbances. Ecosystems 6, 540–550. https://doi.org/10.1007/PL00021507

Pedregosa, F., Varoquaux, G., Gramfort, A., Michel, V., Thirion, B., Grisel, O., Blondel, M., Prettenhofer, P., Weiss, R., Dubourg, V., Vanderplas, J., Passos, A., Cournapeau, D., Brucher, M., Perrot, M., Duchesnay, É., 2011. Scikit-learn: Machine Learning in Python. J. Mach. Learn. Res. 12, 2825–2830.

Ponomarev, E., Yakimov, N., Ponomareva, T., Yakubailik, O., Conard, S.G., 2021. Current Trend of Carbon Emissions from Wildfires in Siberia. Atmosphere 12, 559. https://doi.org/10.3390/atmos12050559

Ponomarev, E.I., Kharuk, V.I., Ranson, K.J., 2016. Wildfires Dynamics in Siberian Larch Forests. Forests 7, 125. https://doi.org/10.3390/f7060125

Potapov, P., Hansen, M.C., Laestadius, L., Turubanova, S., Yaroshenko, A., Thies, C., Smith, W., Zhuravleva, I., Komarova, A., Minnemeyer, S., Esipova, E., 2017. The last frontiers of wilderness: Tracking loss of intact forest landscapes from 2000 to 2013. Sci. Adv. 3, e1600821. https://doi.org/10.1126/sciadv.1600821

Qin, Y., Abatzoglou, J.T., Siebert, S., Huning, L.S., AghaKouchak, A., Mankin, J.S., Hong, C., Tong, D., Davis, S.J., Mueller, N.D., 2020. Agricultural risks from changing snowmelt. Nat. Clim. Change 10, 459–465. https://doi.org/10.1038/s41558-020-0746-8

Randerson, J.T., Chen, Y., Werf, G.R. van der, Rogers, B.M., Morton, D.C., 2012. Global burned area and biomass burning emissions from small fires. J. Geophys. Res. Biogeosciences 117. https://doi.org/10.1029/2012JG002128

Randerson, J.T., van der Werf, G.R., Giglio, L., Collatz, G.J., Kasibhatla, P.S., 2017. Global Fire Emissions Database, Version 4.1 (GFEDv4) 1925.7122549999906 MB. https://doi.org/10.3334/ORNLDAAC/1293

Rogers, B.M., Balch, J.K., Goetz, S.J., Lehmann, C.E.R., Turetsky, M., 2020. Focus on changing fire regimes: interactions with climate, ecosystems, and society. Environ. Res. Lett. 15, 030201. https://doi.org/10.1088/1748-9326/ab6d3a

Rogers, B.M., Soja, A.J., Goulden, M.L., Randerson, J.T., 2015. Influence of tree species on continental differences in boreal fires and climate feedbacks. Nat. Geosci. 8, 228–234. https://doi.org/10.1038/ngeo2352

Sannikov, S.N., Sannikova, N.S., Petrova, I.V., Cherepanova, O.E., 2020. The forecast of fire impact on Pinus sylvestris renewal in southwestern Siberia. J. For. Res. https://doi.org/10.1007/s11676-020-01260-1

Schulze, E.-D., Wirth, C., Mollicone, D., von Lüpke, N., Ziegler, W., Achard, F., Mund, M., Prokushkin, A., Scherbina, S., 2012. Factors promoting larch dominance in central Siberia: fire versus growth performance and implications for carbon dynamics at the boundary of evergreen and deciduous conifers. Biogeosciences 9, 1405–1421. https://doi.org/10.5194/bg-9-1405-2012

Shuman, J.K., Foster, A.C., Shugart, H.H., Hoffman-Hall, A., Krylov, A., Loboda, T., Ershov, D., Sochilova, E., 2017. Fire disturbance and climate change: implications for Russian forests. Environ. Res. Lett. 12, 035003. https://doi.org/10.1088/1748-9326/aa5eed

Shvetsov, E.G., Kukavskaya, E.A., Buryak, L.V., 2016. Satellite monitoring of the state of forest vegetation after fire impacts in the Zabaikal region. Contemp. Probl. Ecol. 9, 702–710. https://doi.org/10.1134/S1995425516060123

Shvetsov, E.G., Kukavskaya, E.A., Buryak, L.V., Barrett, K., 2019. Assessment of post-fire vegetation recovery in Southern Siberia using remote sensing observations. Environ. Res. Lett. 14, 055001. https://doi.org/10.1088/1748-9326/ab083d

Sidoroff, K., Kuuluvainen, T., Tanskanen, H., Vanha-Majamaa, I., 2007. Tree mortality after low-intensity prescribed fires in managed Pinus sylvestris stands in southern Finland. Scand. J. For. Res. 22, 2–12. https://doi.org/10.1080/02827580500365935

Sizov, O., Ezhova, E., Tsymbarovich, P., Soromotin, A., Prihod’ko, N., Petäjä, T., Zilitinkevich, S., Kulmala, M., Bäck, J., Köster, K., 2021. Fire and vegetation dynamics in northwest Siberia during the last 60 years based on high-resolution remote sensing. Biogeosciences 18, 207–228. https://doi.org/10.5194/bg-18-207-2021

Smets, B., Tansey, K., Wolfs, D., Jacobs, T., 2017. PRODUCT USER MANUAL BURNED AREA AND SEASONALITY COLLECTION 300M VERSION 1.

Soja, A., Shugart, H., Sukhinin, A., Conard, S., Stackhouse Jr, P., 2006. Satellite-Derived Mean Fire Return Intervals As Indicators Of Change In Siberia (1995–2002). Mitig. Adapt. Strateg. Glob. Change 11, 75–96. https://doi.org/10.1007/s11027-006-1009-3

Stevens-Rumann, C.S., Kemp, K.B., Higuera, P.E., Harvey, B.J., Rother, M.T., Donato, D.C., Morgan, P., Veblen, T.T., 2018. Evidence for declining forest resilience to wildfires under climate change. Ecol. Lett. 21, 243–252. https://doi.org/10.1111/ele.12889

Suarez, F., Binkley, D., Kaye, M.W., Stottlemyer, R., 1999. Expansion of forest stands into tundra in the Noatak National Preserve, northwest Alaska. Écoscience 6, 465–470. https://doi.org/10.1080/11956860.1999.11682538

Sullivan, Janet., 1993. Pinus sylvestris. [WWW Document]. Fire Eff. Inf. Syst. Online US Dep. Agric. For. Serv. Rocky Mt. Res. Stn. Fire Sci. Lab. Prod. URL https://www.fs.fed.us/database/feis/plants/tree/pinsyl/all.html (accessed 3.5.21).

Tepley, A.J., Thomann, E., Veblen, T.T., Perry, G.L.W., Holz, A., Paritsis, J., Kitzberger, T., Anderson-Teixeira, K.J., 2018. Influences of fire–vegetation feedbacks and post-fire recovery rates on forest landscape vulnerability to altered fire regimes. J. Ecol. 106, 1925–1940. https://doi.org/10.1111/1365-2745.12950

Theil, H., 1950. A rank-invariant method of linear and polynomial regression analysis, Part 3. Presented at the Proceedings of Koninalijke Nederlandse Akademie van Weinenschatpen A, pp. 1397–1412.

Tomshin, O., Solovyev, V., 2021. Spatio-temporal patterns of wildfires in Siberia during 2001–2020. Geocarto Int. 0, 1–19. https://doi.org/10.1080/10106049.2021.1973581

van der Werf, G.R., Randerson, J.T., Giglio, L., van Leeuwen, T.T., Chen, Y., Rogers, B.M., Mu, M., van Marle, M.J.E., Morton, D.C., Collatz, G.J., Yokelson, R.J., Kasibhatla, P.S., 2017. Global fire emissions estimates during 1997–2016. Earth Syst. Sci. Data 9, 697–720. https://doi.org/10.5194/essd-9-697-2017

Walker, X.J., Rogers, B.M., Veraverbeke, S., Johnstone, J.F., Baltzer, J.L., Barrett, K., Bourgeau-Chavez, L., Day, N.J., de Groot, W.J., Dieleman, C.M., Goetz, S., Hoy, E., Jenkins, L.K., Kane, E.S., Parisien, M.-A., Potter, S., Schuur, E. a. G., Turetsky, M., Whitman, E., Mack, M.C., 2020. Fuel availability not fire weather controls boreal wildfire severity and carbon emissions. Nat. Clim. Change 10, 1130–1136. https://doi.org/10.1038/s41558-020-00920-8

Whitman, E., Parisien, M.-A., Thompson, D.K., Flannigan, M.D., 2019. Short-interval wildfire and drought overwhelm boreal forest resilience. Sci. Rep. 9, 1–12. https://doi.org/10.1038/s41598-019-55036-7

Wilks, D.S., 2016. "The Stippling Shows Statistically Significant Grid Points": How Research Results are Routinely Overstated and Overinterpreted, and What to Do about It. Bull. Am. Meteorol. Soc. 97, 2263–2273. https://doi.org/10.1175/BAMS-D-15-00267.1

Wright, J.W., Wilson, L.F., Randall, W.K., 1967. Differences Among Scotch Pine Varieties in Susceptibility to European Pine Sawfly. For. Sci. 13, 175–181. https://doi.org/10.1093/forestscience/13.2.175

Yue, S., Pilon, P., Cavadias, G., 2002. Power of the Mann–Kendall and Spearman's rho tests for detecting monotonic trends in hydrological series. J. Hydrol. 259, 254–271. https://doi.org/10.1016/S0022-1694(01)00594-7

Supplementary Information for:

Climate change, fire return intervals and the growing risk of permanent forest loss in in boreal Eurasia

Arden L. Burrell[1,2*]
Qiaoqi Sun[3,4]
Robert Baxter[3]
Elena A. Kukavskaya[5]
Sergey Zhila[5]
Tatiana Shestakova[1]
Brendan M. Rogers[1]
Kirsten Barrett[2]

1. Woodwell Climate Research Center, Falmouth, MA, United States of America
2. Centre for Landscape and Climate Research, School of Geography, Geology and Environment, University of Leicester, University Road, LE1 7RH, UK
3. Department of Biosciences, University of Durham, Upper Mountjoy, South Road, Durham, DH1 3LE, United Kingdom.
4. College of Wildlife and Protected Area, Northeast Forestry University, 26 Hexing Road, Harbin 150040, China
5. V.N. Sukachev Institute of Forest of the Siberian Branch of the Russian Academy of Sciences - separate subdivision of the FRC KSC SB RAS, 660036 Russian Federation, Krasnoyarsk, Akademgorodok 50/28.

*Corresponding author

Email: aburrell@woodwellclimate.org

This PDF file includes:

Figures S1 to S12

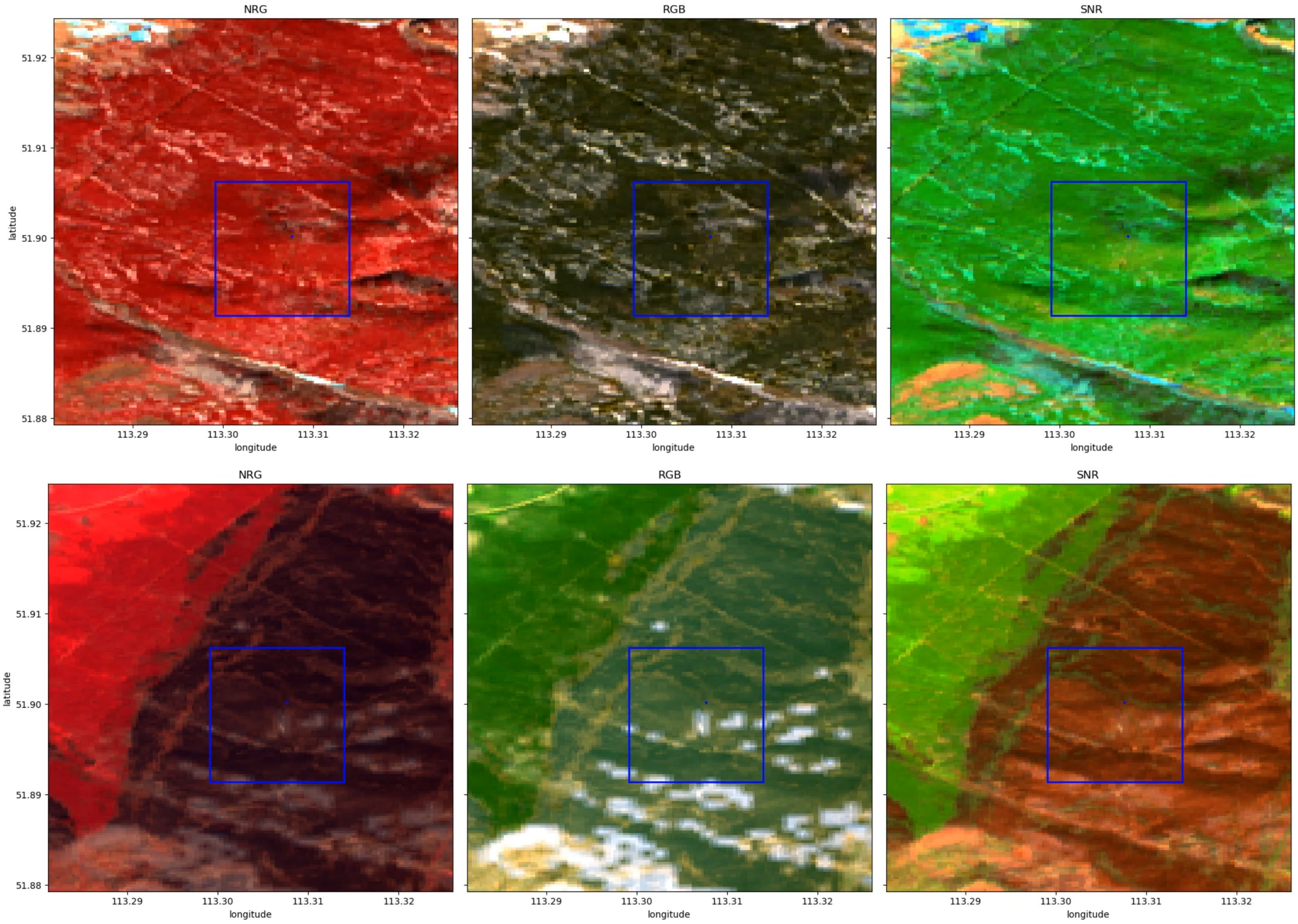

Figure S1 - Example of a 2015 burn at a test site. *NGR is a Near Infrared, Red, Green false-colour image. RGB is the true colour image and SNR is the Shortwave Infrared, Near Infrared, red false-colour image. The blue box is a 1 kmx1 km area around the site that matches the exact grid of the BA datasets and the blue dot in the box is the location of the site. The top row of images are from 2015-03-18 and the bottom row are from 2015-09-08.*

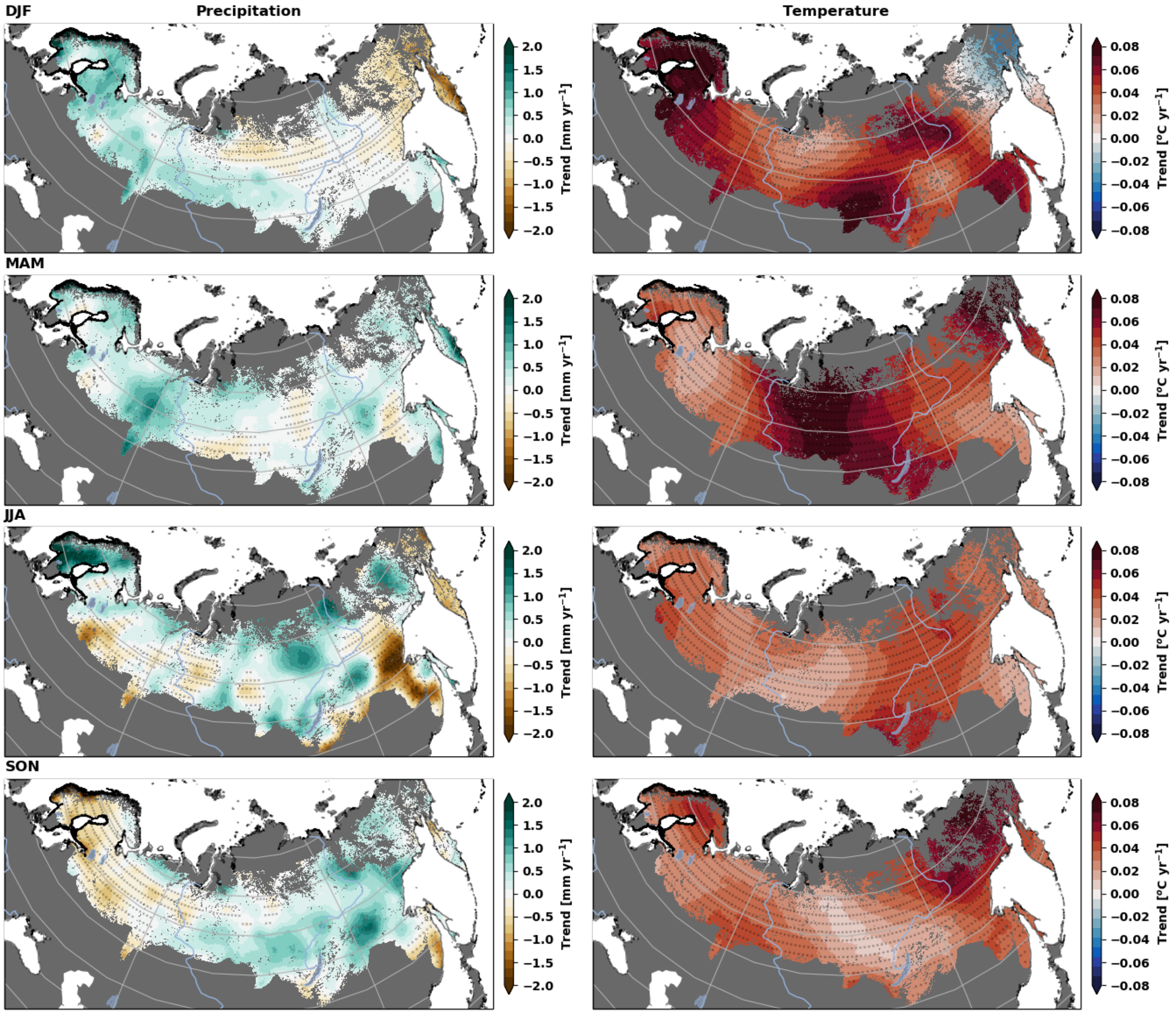

Figure S2 - Climate change driven trends in seasonal accumulated Precipitation and mean Temperature *for the period 1985 to 2015. This figure uses the meteorological seasons December January February (DJF), March April May (MAM), June July August (JJA) and September October November (SON). Non-boreal forest ecosystems are masked in grey and the stippling indicates statistical significance (α_{FDR} = 0.10). Data: TerraClimate (Abatzoglou et al., 2018)*

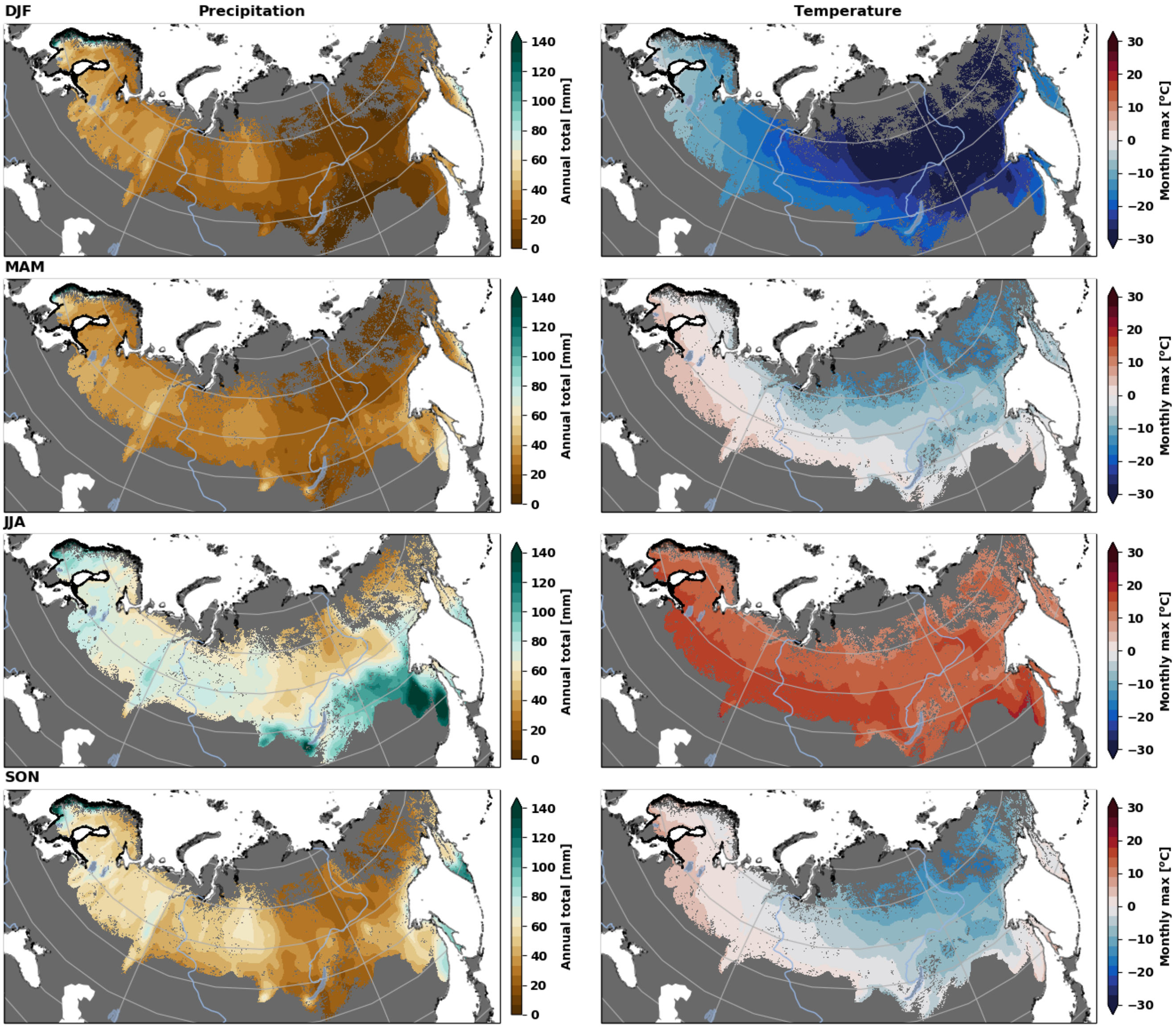

Figure S3 - Mean seasonal climatology *for the period 1985 to 2015. This figure uses the meteorological seasons December January February (DJF), March April May (MAM), June July August (JJA) and September October November (SON). Non-boreal forest ecosystems are masked in grey. Data: TerraClimate (Abatzoglou et al., 2018)*

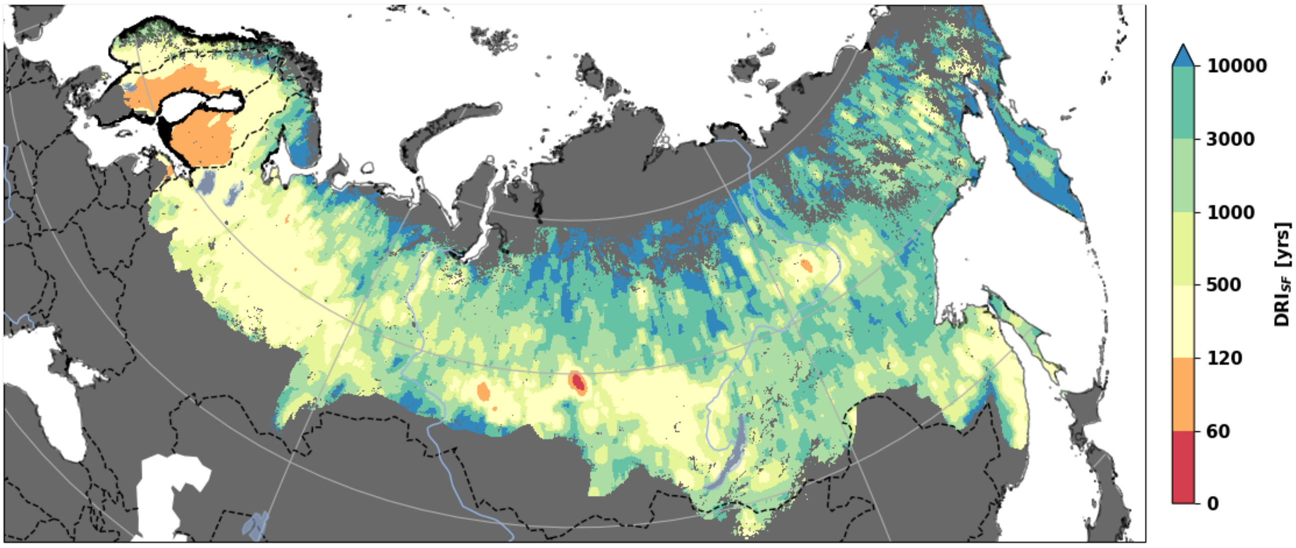

Figure S4 – Disturbance return interval. *The DRI sans fires (DRI$_{SF}$) calculated by removing the forest attributable to fire (HansenGFC-AFM) from the DRI (HansenGFC).*

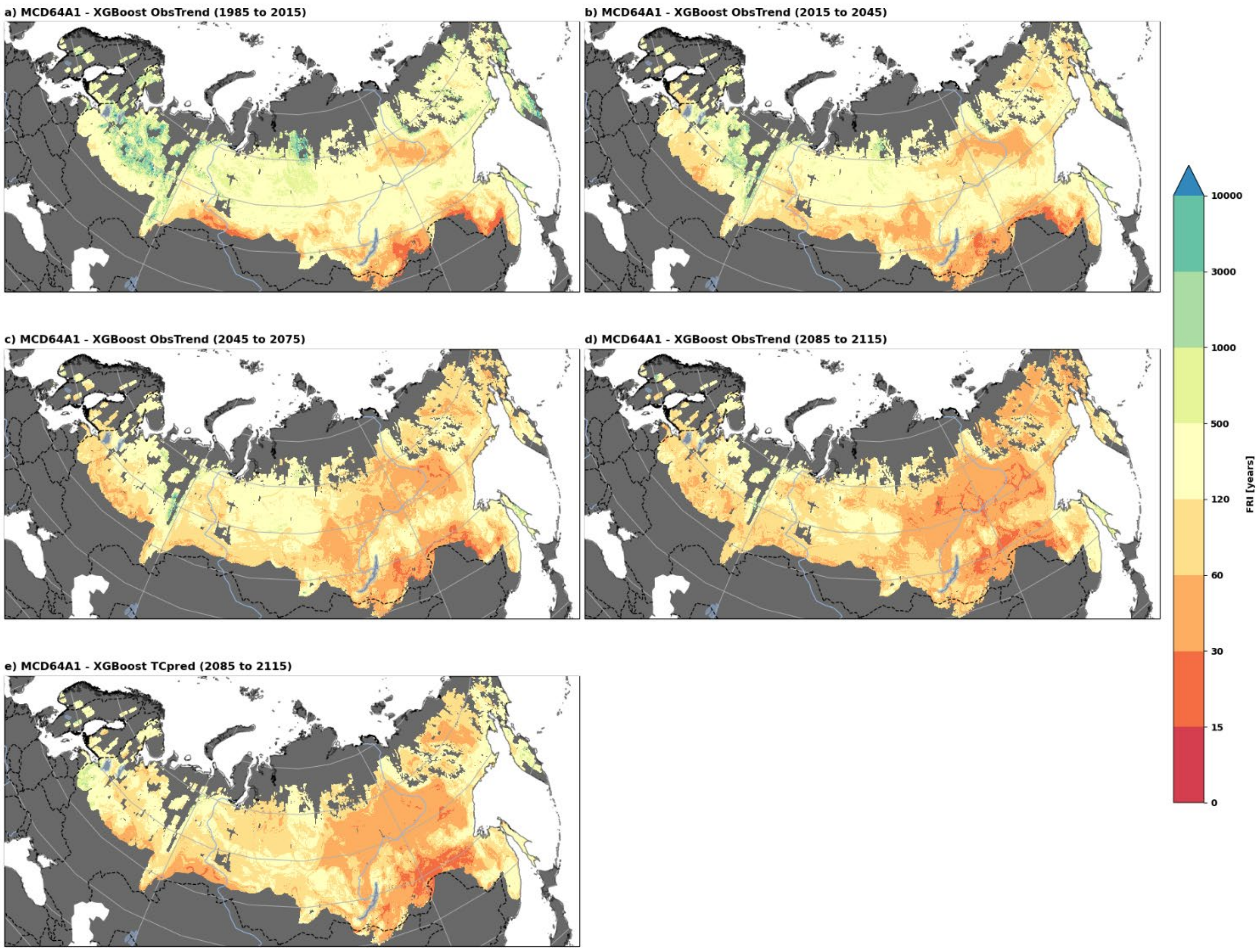

Figure S5 - Maps of the predicted FRI based on current climate trend, XGBoost ML and MCD64A1 FRI data. *TCpred is the Terraclimate prediction for a 4^{0}C warmer world which is approximately SSP3-7.0 2085 – 2115. Non-boreal forest ecosystems are masked in grey.*

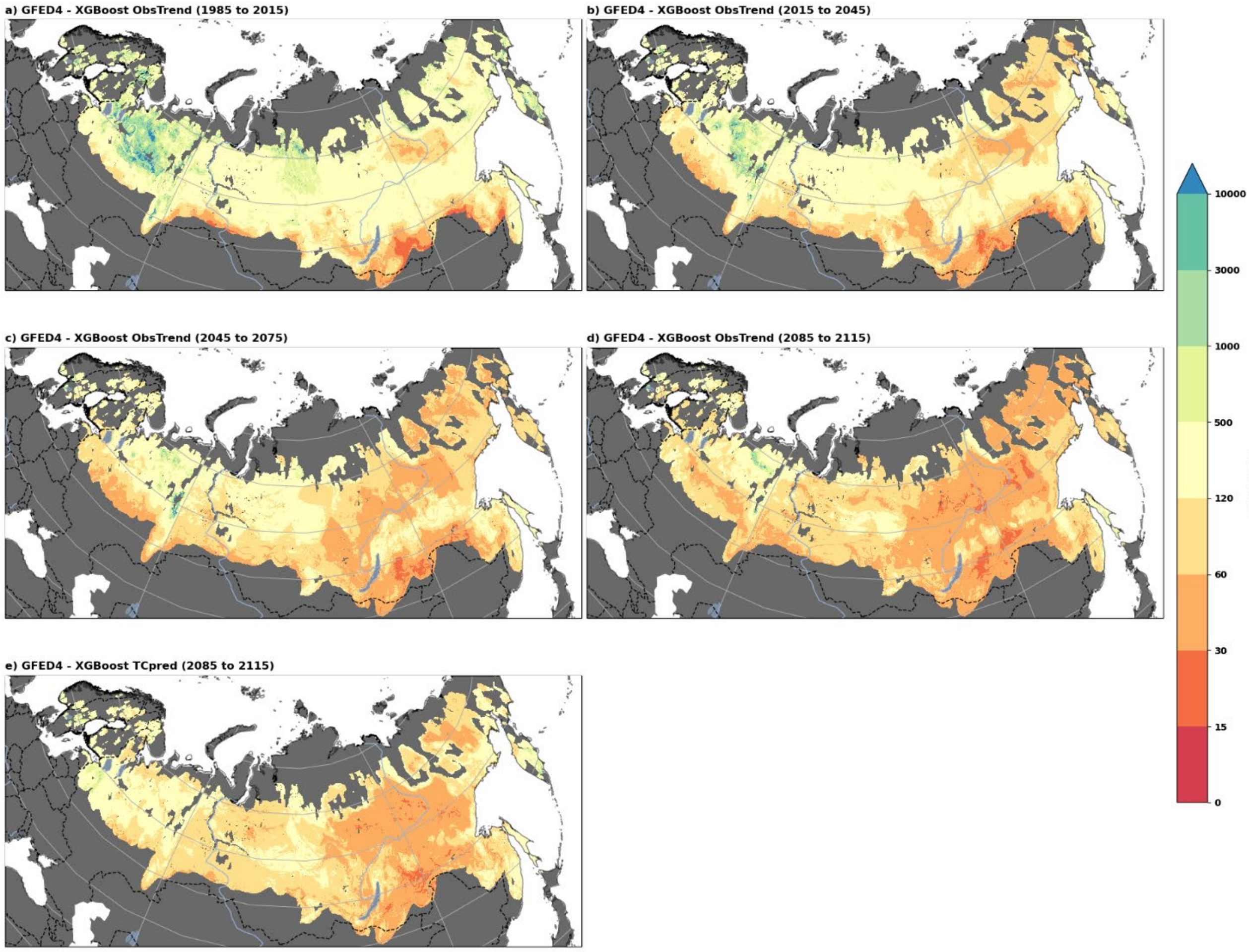

Figure S6 -Maps of the predicted FRI based on current climate trend, XGBoost ML and GFED FRI data. *TCpred is the Terraclimate prediction for a 4^0C warmer world which is approximately SSP3-7.0 2085 – 2115. Non-boreal forest ecosystems are masked in grey.*

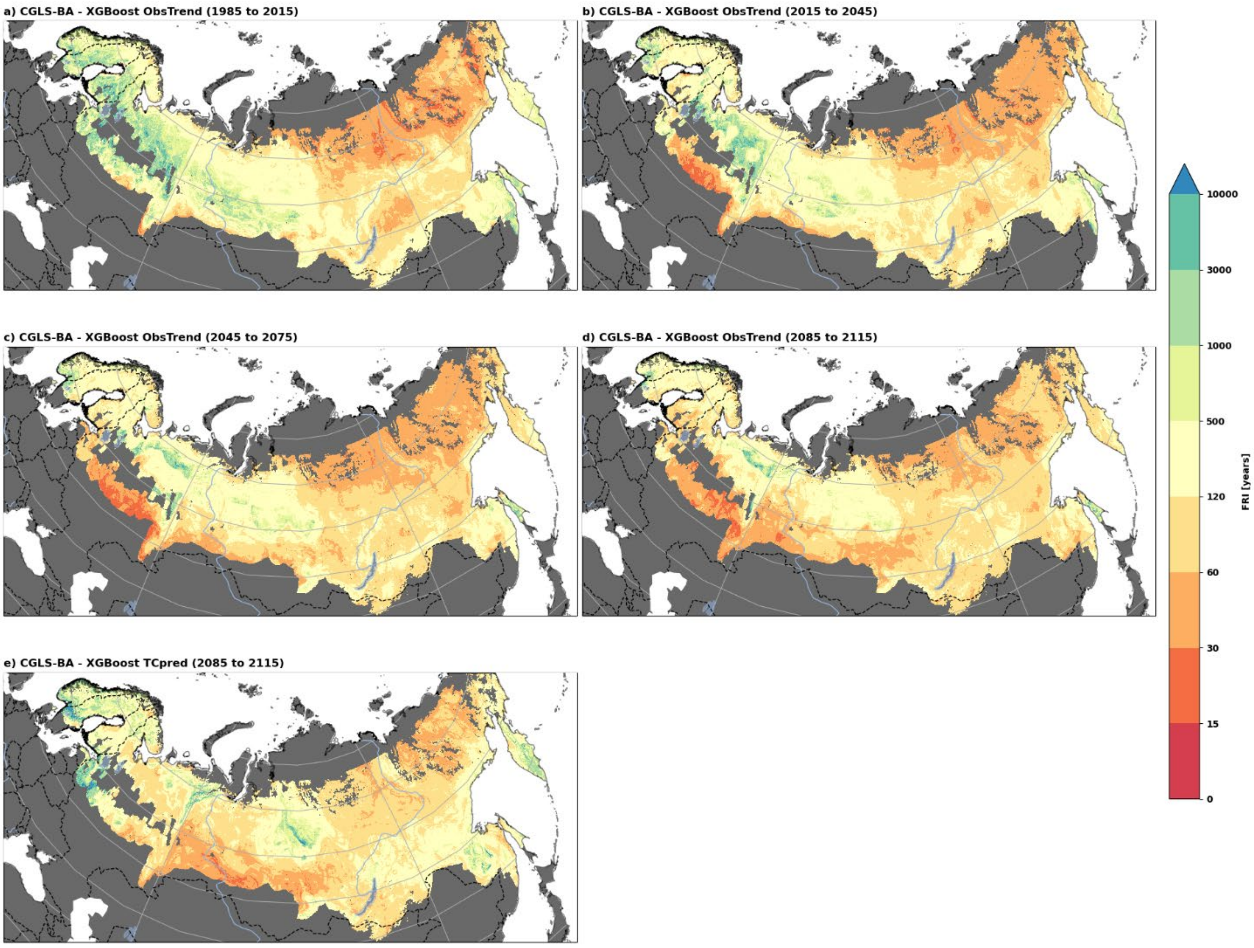

Figure S7 - Maps of the predicted FRI based on current climate trend, XGBoost ML and CGLS-BA FRI data. *TCpred is the Terraclimate prediction for a 4^0C warmer world which is approximately SSP3-7.0 2085 – 2115. Non-boreal forest ecosystems are masked in grey.*

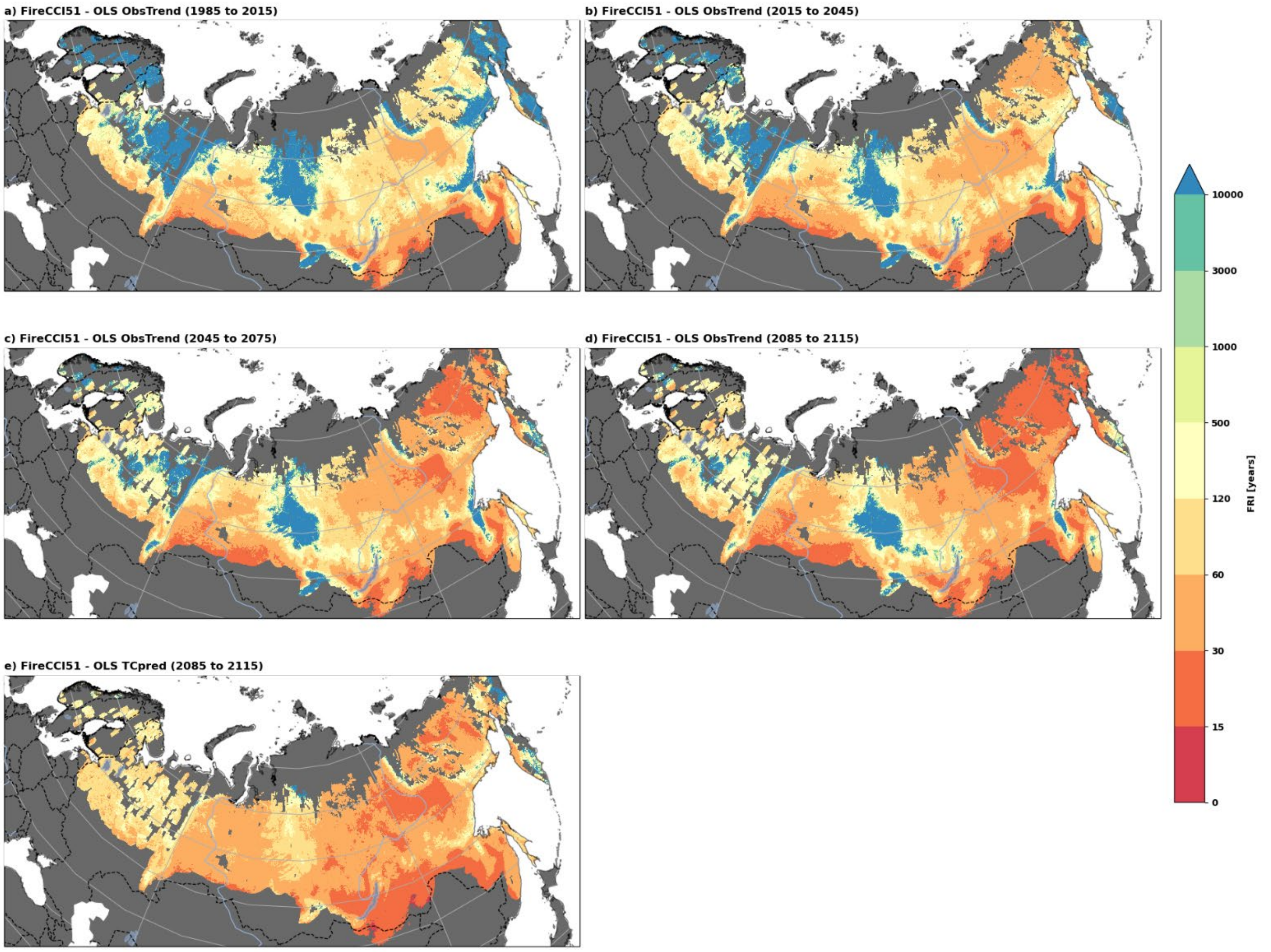

Figure S8 - Maps of the predicted FRI based on current climate trend, OLS and FireCCI51 FRI data. *TCpred is the Terraclimate prediction for a 4^0C warmer world which is approximately SSP3-7.0 2085 – 2115. Non-boreal forest ecosystems are masked in grey.*

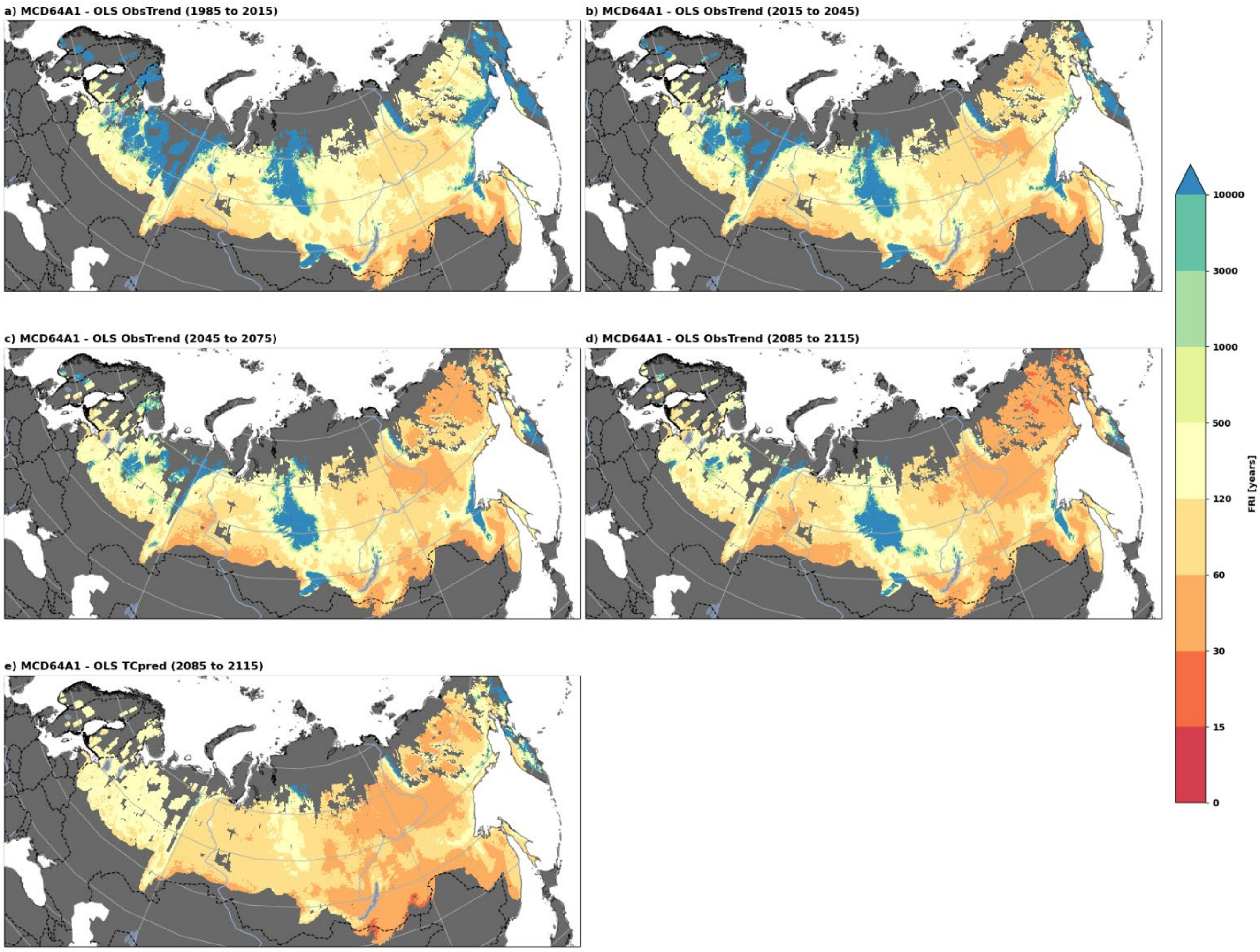

Figure S9 - Maps of the predicted FRI based on current climate trend, OLS and MCD64A1 FRI data. *TCpred is the Terraclimate prediction for a 4^{0}C warmer world which is approximately SSP3-7.0 2085 – 2115. Non-boreal forest ecosystems are masked in grey.*

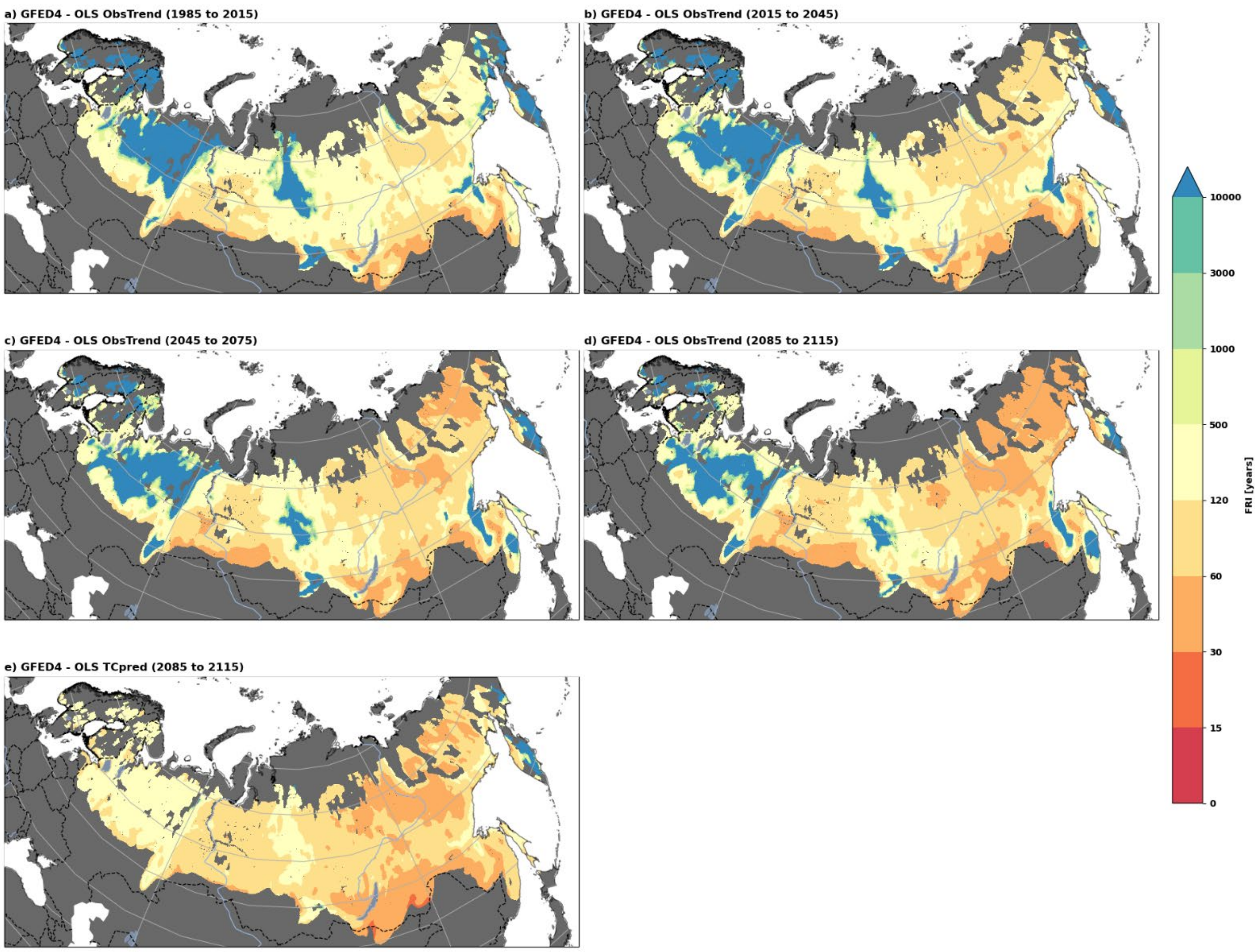

Figure S10 - Maps of the predicted FRI based on current climate trend, OLS and GFED4 FRI data. *TCpred is the Terraclimate prediction for a 4^{0}C warmer world which is approximately SSP3-7.0 2085 – 2115. Non-boreal forest ecosystems are masked in grey.*

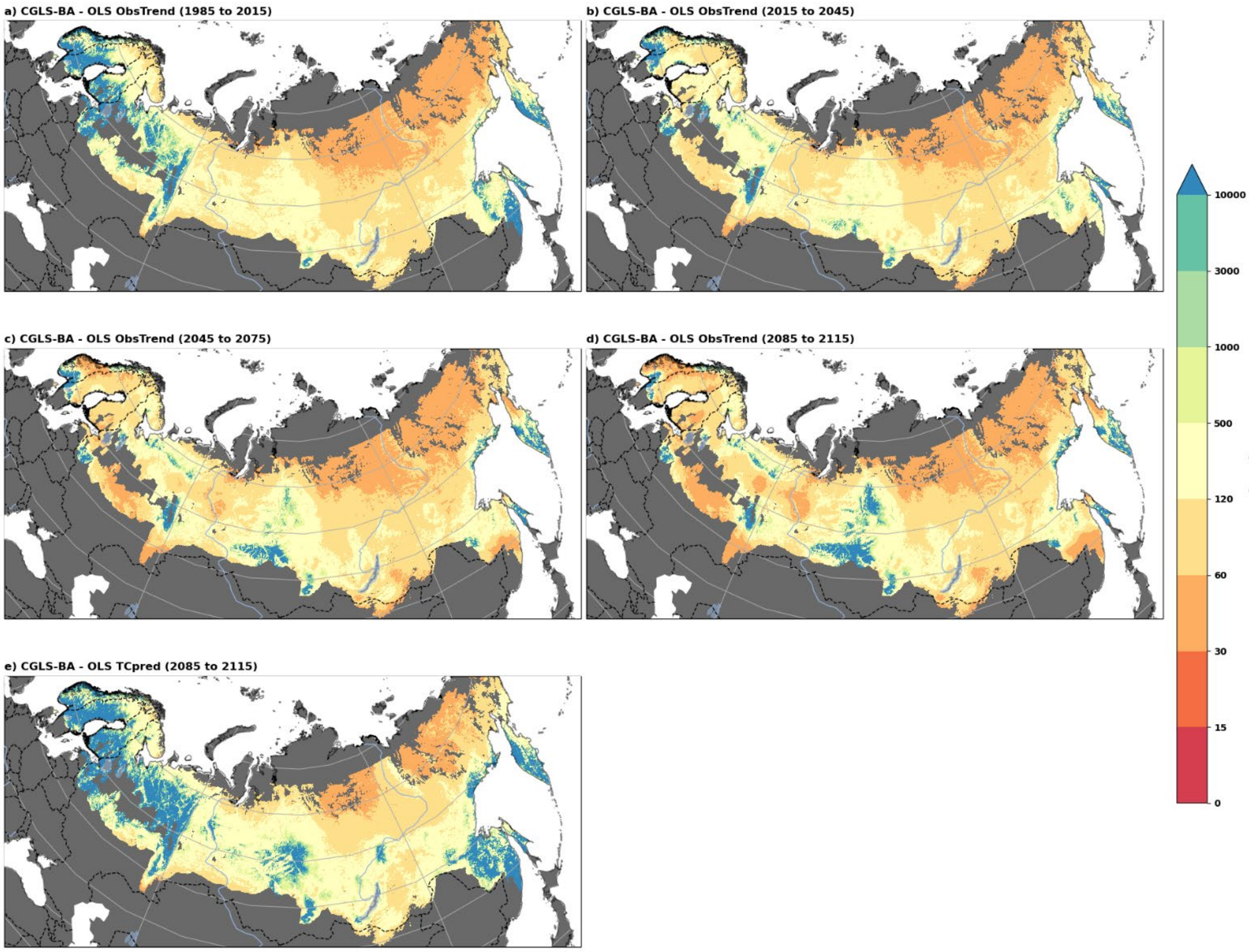

Figure S11 - Maps of the predicted FRI based on current climate trend, OLS and CGLS-BA FRI data. *TCpred is the Terraclimate prediction for a 4^{0}C warmer world which is approximately SSP3-7.0 2085 – 2115. Non-boreal forest ecosystems are masked in grey.*